A European giant: a large spinosaurid (Dinosauria: Theropoda) from the Vectis Formation (Wealden Group, Early Cretaceous), UK (#71640)

First submission

Guidance from your Editor

Please submit by **31 Mar 2022** for the benefit of the authors (and your $200 publishing discount) .

Structure and Criteria
Please read the 'Structure and Criteria' page for general guidance.

Raw data check
Review the raw data.

Image check
Check that figures and images have not been inappropriately manipulated.

Privacy reminder: If uploading an annotated PDF, remove identifiable information to remain anonymous.

Files

Download and review all files from the materials page.

11 Figure file(s)
5 Table file(s)
1 Raw data file(s)
1 Other file(s)

Structure and Criteria

Structure your review

The review form is divided into 5 sections. Please consider these when composing your review:

1. **BASIC REPORTING**
2. **EXPERIMENTAL DESIGN**
3. **VALIDITY OF THE FINDINGS**
4. General comments
5. Confidential notes to the editor

You can also annotate this PDF and upload it as part of your review

When ready submit online.

Editorial Criteria

Use these criteria points to structure your review. The full detailed editorial criteria is on your guidance page.

BASIC REPORTING

- Clear, unambiguous, professional English language used throughout.
- Intro & background to show context. Literature well referenced & relevant.
- Structure conforms to PeerJ standards, discipline norm, or improved for clarity.
- Figures are relevant, high quality, well labelled & described.
- Raw data supplied (see PeerJ policy).

EXPERIMENTAL DESIGN

- Original primary research within Scope of the journal.
- Research question well defined, relevant & meaningful. It is stated how the research fills an identified knowledge gap.
- Rigorous investigation performed to a high technical & ethical standard.
- Methods described with sufficient detail & information to replicate.

VALIDITY OF THE FINDINGS

- Impact and novelty not assessed. *Meaningful* replication encouraged where rationale & benefit to literature is clearly stated.
- All underlying data have been provided; they are robust, statistically sound, & controlled.
- Conclusions are well stated, linked to original research question & limited to supporting results.

Standout reviewing tips

The best reviewers use these techniques

Tip	*Example*
Support criticisms with evidence from the text or from other sources	*Smith et al (J of Methodology, 2005, V3, pp 123) have shown that the analysis you use in Lines 241-250 is not the most appropriate for this situation. Please explain why you used this method.*
Give specific suggestions on how to improve the manuscript	*Your introduction needs more detail. I suggest that you improve the description at lines 57- 86 to provide more justification for your study (specifically, you should expand upon the knowledge gap being filled).*
Comment on language and grammar issues	*The English language should be improved to ensure that an international audience can clearly understand your text. Some examples where the language could be improved include lines 23, 77, 121, 128 – the current phrasing makes comprehension difficult. I suggest you have a colleague who is proficient in English and familiar with the subject matter review your manuscript, or contact a professional editing service.*
Organize by importance of the issues, and number your points	*1. Your most important issue* *2. The next most important item* *3. …* *4. The least important points*
Please provide constructive criticism, and avoid personal opinions	*I thank you for providing the raw data, however your supplemental files need more descriptive metadata identifiers to be useful to future readers. Although your results are compelling, the data analysis should be improved in the following ways: AA, BB, CC*
Comment on strengths (as well as weaknesses) of the manuscript	*I commend the authors for their extensive data set, compiled over many years of detailed fieldwork. In addition, the manuscript is clearly written in professional, unambiguous language. If there is a weakness, it is in the statistical analysis (as I have noted above) which should be improved upon before Acceptance.*

A European giant: a large spinosaurid (Dinosauria: Theropoda) from the Vectis Formation (Wealden Group, Early Cretaceous), UK

Chris T Barker Corresp., 1, 2 , **Jeremy A. F. Lockwood** 3, 4 , **Darren Naish** 5 , **Sophie Brown** 5 , **Amy Hart** 5 , **Ethan Tulloch** 5 , **Neil J Gostling** Corresp. 1, 5

1 Institute for Life Sciences, University of Southampton, Southampton, United Kingdom
2 Faculty of Engineering and Physical Sciences, University of Southampton, Southampton, United Kingdom
3 School of Environment, Geography and Geosciences, University of Portsmouth, Portsmouth, United Kingdom
4 Department of Earth Sciences, Natural History Museum, London, United Kingdom
5 School of Biological Sciences, University of Southampton, Southampton, United Kingdom

Corresponding Authors: Chris T Barker, Neil J Gostling
Email address: ctb1g14@soton.ac.uk, n.j.gostling@soton.ac.uk

Postcranial elements (cervical, sacral and caudal vertebrae, as well as ilium, rib and limb bone fragments) belonging to a gigantic tetanuran theropod were recovered from the basal unit (the White Rock Sandstone) of the Vectis Formation near Compton Chine, on the southwest coast of the Isle of Wight. These remains appear to pertain to the same individual, with enormous dimensions similar to those of the *Spinosaurus* holotype and exceeding those of the largest European theropods previously reported. A combination of features, including the presence of spinodiapophyseal webbing on an anterior caudal vertebra, suggest that this is a member of Spinosauridae, though a lack of convincing autapomorphies precludes the identification of a new taxon. Phylogenetic analysis supports spinosaurid affinities but of indeterminate position within the clade, though weak support for a position within Spinosaurinae or an early-diverging position within Spinosauridae was found in some data runs. This is the first spinosaurid reported from the Vectis Formation and the youngest British material referred to the clade. This Vectis Formation spinosaurid is unusual in that the majority of dinosaurs from the Lower Cretaceous units of the Wealden Supergroup are from the fluviolacustrine deposits of the underlying Barremian Wessex Formation. In contrast, the lagoonal facies of the upper Barremian–lower Aptian Vectis Formation only rarely yield dinosaur material. Our conclusions are in keeping with previous studies that emphasise western Europe as a pivotal region within spinosaurid origination and diversification.

A European giant: a large spinosaurid (Dinosauria: Theropoda) from the Vectis Formation (Wealden Group, Early Cretaceous), UK.

Chris T. Barker[1,2], Jeremy A. F. Lockwood[3, 4], Darren Naish[5], Sophie Brown[5], Amy Hart[5], Ethan Tulloch[5], Neil J. Gostling[1,5]

[1]Institute for Life Sciences, University of Southampton, University Road, Southampton, SO17 1BJ, UK
[2]Faculty of Engineering and Physical Sciences, University of Southampton, University Road, Southampton, SO17 1BJ, UK
[3]School of Environment, Geography and Geosciences, University of Portsmouth, Burnaby Road, Portsmouth, PO1 3QL, UK
[4]Department of Earth Sciences, Natural History Museum, Cromwell Road, London SW7 5BD, UK
[5]School of Biological Sciences, Faculty of Environment and Life Sciences, University of Southampton, University Road, Southampton, SO17 1BJ, UK

Corresponding Author:
Dr. Neil J. Gostling
Institute for Life Sciences, University of Southampton, University Road, Southampton, SO17 1BJ, UK
Email address: N.J.Gostling@soton.ac.uk

Abstract

Postcranial elements (cervical, sacral and caudal vertebrae, as well as ilium, rib and limb bone fragments) belonging to a gigantic tetanuran theropod were recovered from the basal unit (the White Rock Sandstone) of the Vectis Formation near Compton Chine, on the southwest coast of the Isle of Wight. These remains appear to pertain to the same individual, with enormous dimensions similar to those of the *Spinosaurus* holotype and exceeding those of the largest European theropods previously reported. A combination of features, including the presence of spinodiapophyseal webbing on an anterior caudal vertebra, suggest that this is a member of Spinosauridae, though a lack of convincing autapomorphies precludes the identification of a new taxon. Phylogenetic analysis supports spinosaurid affinities but of indeterminate position within the clade, though weak support for a position within Spinosaurinae or an early-diverging position within Spinosauridae was found in some data runs. This is the first spinosaurid reported from the Vectis Formation and the youngest British material referred to the clade. This Vectis Formation spinosaurid is unusual in that the majority of dinosaurs from the Lower Cretaceous units of the Wealden Supergroup are from the fluviolacustrine deposits of the underlying Barremian Wessex Formation. In contrast, the lagoonal facies of the upper Barremian–lower Aptian Vectis Formation only rarely yield dinosaur material. Our conclusions are in keeping with previous studies that emphasise western Europe as a pivotal region within spinosaurid origination and diversification.

Introduction

The deposits of the internationally important Wessex Formation of the Isle of Wight – part of the Wealden Group (itself part of the Wealden Supergroup) – have been and remain exceptionally productive regarding dinosaur material and research (Insole & Hutt 1994; Radley & Allen 2012c; Sweetman 2011). Indeed, the Wessex Formation has yielded almost all dinosaur fossils known from the Isle of Wight (Martill & Naish 2001b). Its fluviolacustrine sediments preserve the remains of various tetanuran theropods, rebbachisaurid and titanosauriform sauropods, and a variety of ornithischians, including ankylosaurs and ornithopods (Benton & Spencer 1995; Lomax & Tamura 2014; Martill & Naish 2001a; Naish & Martill 2007; Naish & Martill 2008). In contrast, dinosaur remains are rare in the overlying Vectis Formation (Radley et al. 1998), documented finds being limited to a handful of ornithopod, ankylosaur and indeterminate theropod specimens (Benton & Spencer 1995; Blows 1987; Hooley 1925; Martill & Naish 2001a; Naish & Martill 2008; Weishampel et al. 2004; White 1921). Ichnological remains referred to theropod, thyreophoran and ornithopod track-makers have also been reported from the Vectis Formation (Pond et al. 2014; Radley et al. 1998).

A number of large, fragmentary dinosaur bones, encased in a matrix matching the basal unit (the White Rock Sandstone) of the Vectis Formation, were found east of Compton Chine on the southwest coast of the Isle of Wight by Mr Nick Chase and Dr Jeremy Lockwood over a period of several months. Taphonomic and anatomical evidence (discussed below) show that they belong to a single individual. Some of these bones were figured and alluded to in Austen & Batten (2018) but they have not previously been described. A list of character traits show that the specimen likely belongs to Spinosauridae and is thus the first member of this clade reported from the Vectis Formation. The specimen's large size is noteworthy and it appears to represent the largest theropod yet reported from the Wealden Supergroup and potentially from the European fossil record in general.

Our identification of this specimen as a spinosaurid is interesting in view of recent discoveries pertaining to spinosaurid diversity within the Wealden Supergroup. Spinosauridae is characterised by atypical cranial (and sometimes postcranial) morphologies indicative of divergent, semi-aquatic ecologies relative to related lineages (Amiot et al. 2009; Amiot et al. 2010; Aureliano et al. 2018; Charig & Milner 1997; Hassler et al. 2018; Ibrahim et al. 2020a; Ibrahim et al. 2014; McCurry et al. 2019). Most studies support the division of Spinosauridae into Baryonychinae and Spinosaurinae (Arden et al. 2019; Benson 2010; Carrano et al. 2012; Rauhut & Pol 2019; Sereno et al. 1998), although there are indications that support for this dichotomy may be weaker than customarily supposed (Barker et al. 2021; Evers et al. 2015). Most spinosaurids hail from Early and "mid" Cretaceous strata but phylogenetic analyses support a Jurassic origin for the clade (Barker et al. 2021; Hone & Holtz Jr 2017) and isolated teeth suggest spinosaurid persistence into the Late Cretaceous (Santonian) (Hone et al. 2010). To date, all formally published British spinosaurid remains come from the Berriasian–lower Aptian Wealden Supergroup, and include *Baryonyx walkeri* from the Upper Weald Clay Formation of the Weald sub-basin (Charig & Milner 1986; Charig & Milner 1997), and *Ceratosuchops inferodios* and *Riparovenator milnerae* from the Wessex Formation of the Wessex sub-basin (Barker et al. 2021). Additional fragmentary material has been recovered throughout the Wealden succession (Buffetaut 2010; Charig & Milner 1997; Hutt & Newbery 2004; Martill & Hutt 1996; Milner 2003; Naish et al. 2001; Salisbury & Naish 2011; Turmine-Juhel et al. 2019). This Wealden Supergroup material pertains exclusively to Baryonychinae and spinosaurines are currently unknown from the British fossil record. This contrasts with equivalent strata in Iberia, where evidence of both clades is known (see Malafaia et al. (2020a) for a review of the Iberian spinosaurid record).

In the present contribution, we provide osteological descriptions and comparisons of the better-preserved remains (several additional fragments, including some large pieces, could not be readily identified but are briefly reported in the supplementary information), and include the White Rock spinosaurid in a phylogenetic analysis in order to further test its affinities.

Geological Context

The Wealden Supergroup of southern England is a succession of largely non-marine strata accumulated during the Early Cretaceous (late Berriasian–early Aptian) and mainly deposited in two sub-basins (Fig. 1A): the larger Weald sub-basin of south-eastern England, and the smaller Wessex sub-basin of the Isle of Wight and central-southern England (Batten 2011; Radley & Allen 2012a).

Within the latter, the succession consists of the younger Wealden Group and older Purbeck Limestone Group. The Wealden Group on the Isle of Wight (Fig. 1B) predominantly crops out along the island's southwest coast, with a smaller exposure occurring along the southeast coast. Both areas reveal the entirely Barremian and predominately alluvial facies of the Wessex Formation (deposited in a fluviolacustrine setting) as well as the overlying late Barremian–early Aptian Vectis Formation (Radley & Allen 2012c; Sweetman 2011) (Fig. 1C).
The three constituent members of the 67 m thick Vectis Formation represent the return to coastal lagoonal environments that occurred prior to the Aptian marine transgression and are characterised by low diversity ostracod and mollusc assemblages (Radley et al. 1998; Sweetman 2011). The largely argillaceous Cowleaze Chine and Shepherd's Chine members form the base and top of the formation respectively, denoting low-energy subaqueous or mudflat environments. The Barremian–Aptian boundary occurs within the Shepherd's Chine Member (Kerth & Hailwood 1988; Robinson & Hesselbo 2004). The interceding Barnes High Sandstone Member represents deltaic inundation into the lagoon (Radley et al. 1998).

At the Atherfield type locality and extending west of Cowleaze Chine, a pale, metre-thick sandstone unit in-fills the "dinoturbated" uppermost stratum (the *Hypsilophodon* bed) of the underlying Wessex Formation and forms the base of the Cowleaze Chine Member (Radley et al. 1998; Sweetman 2011). Known as the White Rock Sandstone, it is interpreted as narrow fluvial channels intersecting a marginal lagoonal sand-flat deposit laid down by climatically-controlled terrestrial runoff and intermittent lagoonal influxes (Radley et al. 1998; Sweetman 2011). The lower part of the White Rock Sandstone is formed of laminated, cross-laminated or burrow-mottled sandstone (Radley et al. 1998). Lenses of fusain-rich carbonaceous sandstone, organic-rich mudstones, and poorly sorted conglomerate are interspersed throughout this lower part; the conglomerates occasionally yield worn reptilian bone fragments (Radley et al. 1998).
Due to a fault, the Vectis Formation crops out at two sites in Compton Bay, the larger exposure being located to the east near Shippards Chine and the other towards the west, nearer Compton Chine (Fig. 2A). The specimens were all found in front of the ~34 m thick (Radley & Allen 2012c) more western exposure, along an approximately 50 m stretch of foreshore. Here, the basal ~60 cm unit of the Vectis Formation is lithologically variable and includes a fine sandstone and a pale jarositic siltstone, resembling the higher part of the White Rock Sandstone at the previously described type locality, and is marked at the outcrop by a line of water seepage (Radley & Barker 1998). This White Rock Sandstone equivalent forms an obvious layer that is distinct from the dark grey mud and siltstones of the lagoonal sediments of the Cowleaze Chine member and the varicoloured palaeosols or grey plant debris beds of the Wessex Formation (Fig. 2B). Although all the spinosaurid specimens reported here were found on the foreshore, adhering

matrix closely matches that of the White Rock Sandstone equivalent, and the remains were likely present on the foreshore due to a cliff fall, though the possibility remains that their presence is due to erosion through a wave cut platform (Fig. 2C). Generally, the White Rock equivalent at this location contains few macroscopic fossils except for sporadic fragments of fusain and bone. Ichnites are represented by the occasional gastrolith and infrequent burrows usually ~1 cm in diameter.

Materials & Methods

Measurements

Measurements were taken in millimetres using digital callipers and rounded to one decimal point.

Terminology

Nomenclature of the vertebral neural arch fossae and laminae follows Wilson *et al*. (2011), whilst those of the sacral anatomy follow Wilson (2011). Relative position within the axial series is based on the suggestions of Evers *et al*. (2015) and we also follow the latter authors in their repositioning of the *Baryonyx walkeri* type presacral series. Nomenclature of the various ichnological features found on these specimens follows the ichnotaxobases provided by Pirrone *et al*. (2014).

Phylogenetic Analysis

The White Rock spinosaurid was included in a comprehensive phylogenetic matrix derived from Cau (2018) and implemented in Barker *et al.* (2021), focusing on non-coelurosaurian tetanurans. Following our positional identifications (see "Descriptive osteology"), IWCMS 2018.30.1 was scored as an anterior dorsal vertebra, whilst IWCMS 2018.30.3 was scored as an anterior caudal vertebra.

Scores for five character statements concerning the two operational taxonomic units (OTUs) *Baryonyx* (NHMUK PV R 9951) and *Riparovenator* were changed relative to the analysis in Barker *et al*. (2021). For *Baryonyx*, these changes related to the caudal neural arch characters (Ch.) 358, 359, 868 and 1576. An isolated neural arch belonging to NHMUK PV R 9951 was identified as that of an anterior caudal vertebra by Charig & Milner (1997). However, the presence of a hyposphene and well-developed centrodiapophyseal laminae alternatively suggest that the element instead belongs to a posterior dorsal vertebra, an identification also proposed by Charig & Milner (1997). Given this uncertainty, we opt to re-code the above character as "?". Regarding *Riparovenator*, Ch. 1035 (originally Ch. 99 of (Carrano & Sampson 2008) and concerning caudal neural spine morphology) was mis-scored and has been changed to state 1 to reflect their abbreviated state. All other scores and specimens remained the same as in the Barker *et al.* (2021) analysis, although we acknowledge the recent designation of the specimen ML 1190 as the holotype of the new spinosaurid taxon *Iberospinus natarioi* (Mateus & Estraviz-López 2022), which also includes some fragmentary new material.

The final matrix contains 41 operational taxonomic units coded for 1810 binary character statements. The analysis was performed in TNT v1.5 (Goloboff & Catalano 2016). A driven search using 100 initial addition sequences was performed via the "New Technology Search" function, with default settings employed for sectorial, ratchet, drift and fusion. Tree islands were further explored via a round of tree bisection and reconnection (TBR) using the "Traditional search" function. The identification of wildcard taxa was performed using the iterPCR method (Pol & Escapa 2009) implemented in TNT (Trees>Comparisons). Bremer (decay indices) were employed as measure of absolute tree support, retaining trees suboptimal by 10 steps.

Results

Theropod affinity of the material

Multiple lines of evidence suggest the material pertains to a large theropod dinosaur. Whilst the neural arch fossae and delimiting laminae support the saurischian affinities of IWCMS 2018.30.3 more generally (Wilson et al. 2011), the presence of a pneumatic foramen posterior to the parapophysis supports theropodan or neotherapodan affinities of the anterior presacral vertebra IWCMS 2018.30.1 (Carrano et al. 2012; Cau 2018). The opisthocoelous condition of the latter's centrum (Holtz et al. 2004) is common within the cervical and anterior dorsal vertebrae of non-coelurosaurian tetanurans; indeed, opisthocoely is synapomorphic of carnosaur cervicals in certain analyses (Rauhut 2003; Rauhut & Pol 2019) and is notably pronounced in allosauroids and megalosauroids (Evers et al. 2015). Elsewhere, the pronounced, well-developed brevis fossa of the ilium has been considered diagnostic of Theropoda in some previous works (Gauthier 1986), although a large and expanded brevis fossa on the ilium is observed for dinosaurs more generally (Hutchinson 2001). Also of note is the relatively thin-walled nature of the long bones fragments, a trait also deemed synapomorphic for Theropoda (Gauthier 1986).

Sauropods share opisthocoelous and pneumatic cervical and anterior dorsal vertebrae with some theropods (Upchurch et al. 2004; Upchurch et al. 2011) but several lines of evidence are inconsistent with a sauropod identity for the Compton Chine material. If a cervical position is assumed for IWCMS 2018.30.1 (see "Descriptive osteology" for further comments regarding element position), subdivision of the pneumatic foramen would be expected (Upchurch 1995; Whitlock 2011). Moreover, cervical ventral keels are rare in sauropods and their parapophyses – which are typically indented – consistently maintain a ventral position throughout the series (Upchurch et al. 2004). Similarly, if an anterior dorsal position is assumed, the element's generally abbreviated dimensions are inconsistent with a sauropod identity, since these vertebrae are the longest of the dorsal series in Sauropoda (Upchurch et al. 2004). In addition, while opisthocoelous and ventrally keeled cervical and anterior dorsal vertebrae are present in large ornithopod vertebrae from the Wealden Supergroup (Norman 2011), skeletal pneumaticity is absent within Ornithischia (Rauhut 2003). Further, the proposed caudal element IWCMS 2018.30.3 lacks the ossified tendons present on the neural spines of ornithopod vertebrae near the pelvis (Norman 2011), and lacks the rectangular outline of the anterior caudal vertebrae of basal iguanodontians (Norman 2004). Referral to either Sauropoda or Ornithopoda can thus be rejected.

More specifically, the flattened peripheral rim around the anterior articular surface observed in IWCMS 2018.30.1 is characteristic of megalosaurian cervical vertebrae (Carrano et al. 2012), although it can be observed in anterior dorsal vertebrae as well (e.g. *Baryonyx*; Charig & Milner (1997). Additionally, the presence of spinodiapophyseal webbing in IWCMS 2018.30.3 is characteristic of spinosaurid dorsal vertebrae (or various spinosaurid in-groups, depending on the analysis) (Barker et al. 2021; Benson 2010; Carrano et al. 2012; Evers et al. 2015; Holtz et al. 2004; Rauhut 2003; Rauhut & Pol 2019) and have been documented in spinosaurid anterior caudal vertebrae as well (Barker et al. 2021; Samathi et al. 2021). Coria & Currie (2016) described the presence of webbing in the dorsals of some megaraptorans, although the clade currently lacks any presence in the European record (White et al. 2020). Thus, combined with our phylogenetic results (see Phylogenetic Analysis), we consider the presently discussed material to pertain to a large spinosaurid.

Phylogenetic analysis

The New Technology Search returned 30 trees of 2451 steps and consistency, rescaled consistency, and retention indices (CI, RCI and RI) of 0.493, 0.223 and 0.456 respectively. The round of TBR recovered 22535 trees. The strict consensus tree finds Spinosauridae to be completely unresolved (Fig. 3A). Interestingly, the maximum agreement subtree recovered a baryonychine-spinosaurine split, with the White Rock spinosaurid placed as an early-branching member of Spinosaurinae (Fig. 3B). Three characters were shared between the White Rock spinosaurid and other spinosaurines, all from the anterior caudal series: the presence of centrodiapophyseal laminae (Ch. 358:1), the presence of prezygodiapophyseal laminae (Ch. 626:1), and the presence of a deep prezygocentrodiapophyseal fossa (Ch. 1605:1). Seven other spinosaurid OTUs (*Irritator*, MSNM V4047, *Sigilmassasaurus*, '*Spinosaurus* B', ML 1190, *Vallibonavenatrix* and *Camarillasaurus*) were identified as wildcard taxa following the iterPCR method. Jackknife resampling (Fig. 3C) was unable to recover a spinosaurine position however, with the White Rock spinosaurid instead assuming a polytomous position within Spinosauridae.

Descriptive osteology

Axial elements

IWCMS 2018.30.1 (Probable anterior dorsal vertebra)

This element is represented by the majority of the centrum and a portion of the right neural arch (Fig. 4), metric data of which are presented in Table 1. The left side of the anterior and posterior articular facets are substantially abraded, as is the ventral rim of the anterior facet, exposing cancellous bone and its trabeculae; this ventral abrasion has also affected the anterior part of the ventral keel. A sub-circular portion of the bone has been lost from the right ventral surface, incorporating a part of the ventral keel. The extensive damage to the neural arch and loss of most of its structures has also exposed cancellous bone across the dorsal surface, as well as on the floor of the wide neural canal. The specimen has likely experienced some plastic deformation; given the posterolaterally facing rather than laterally facing parapophysis, this deformation may be related to compressive forces.

The anteroposteriorly abbreviated centrum is opisthocoelous, with a pronounced anterior convexity and posterior concavity. The nature of the neurocentral suture is ambiguous; a suture-like feature is visible in anterior and lateral view and located above the parapophysis, suggesting the latter is thus entirely centrum-bound if genuine. However, this structure may be a taphonomic artefact and not a suture at all.

Both articular facets are mediolaterally wide and in line with one another (i.e. the anterior facet is not dorsally offset relative to the posterior facet); the posterior facet protrudes lateral to the extremities of the anterior equivalent when the specimen is viewed dorsally. The anterior facet lacks any notable inclination but is not uniformly convex since a subtle, median tuberosity is present. This tuberosity is visible in lateral view and protrudes a short distance anteriorly (Fig. 4A). The dorsal margin of the anterior facet is subtly concave dorsal to the tuberosity, such that the dorsal margin is indented in anterior view. A distinct flattened rim is present on the undamaged dorsal portion of the right side of the facet, demarcated posteriorly by a low ridge. The concave right lateral surface possesses a sediment-filled pneumatic foramen, located posteroventral to the ipsilateral parapophysis. The original shape of the foramen cannot be ascertained, and damage precludes identification of the foramen on the left side. The foramen appears to communicate with a shallow yet broad sulcus that cuts into the centrum ventral to the parapophysis (Fig. 4A). The parapophysis is sub-circular and largely flattened.

Ventrally, the centrum possesses a stout keel, which is better developed anteriorly. A ventral fossa on the left side of the centrum contributes somewhat to the keel's pronounced nature, although this is not mirrored on the right. The posterior portion of the keel expands mediolaterally as it becomes confluent with the posterior articular margin.

Regarding its position within the axial series, the anterodorsal location of the parapophysis, sub-parallel (rather than offset) relationship between the articular facets, and possession of a prominent ventral keel (Evers et al. 2015) suggest a cervico-dorsal identity. The position of the parapophysis implies a cervical or anterior dorsal position since tetanuran parapophyses typically migrate onto the neural arch between the 2nd and 7th dorsal (Holtz et al. 2004). The position of the parapophysis in IWCMS 2018.30.1 is most similar to the second dorsal vertebrae of *Baryonyx* (NHMUK PV R9951; fourth dorsal of Charig & Milner (1997) and second and third dorsals of cf. *Suchomimus* (MNBH GAD70, Ibrahim *et al.* (2020b): Figure 130). For this reason, we favour its identification as an anterior dorsal vertebra.

IWCMS 2018.30.2 (Sacral vertebrae)

Two sacral centra, fused at their intercentral junction, are known (Fig. 5): the centra are relatively well preserved, but the neural arches and sacral ribs are missing. The only damage consists of shallow cracks on the smooth external surfaces of the centra, and a large oblique transverse crack near the posterior articular facet of the more posterior centrum. Abrasion has damaged most surfaces to some extent, but most notably affects the parapophyses as well as both articular facets and the conjoined intercentral junction, where the underlying trabeculae are exposed. An indeterminate mass of bone and matrix is cemented onto the floor of the neural canal of the more posterior centrum. Metric data are presented in Table 2.

The ~~robust~~ centra are robust and longer than tall, and are approximately in line with one another. The exposed hemielliptical anterior facet of the anterior element is flat and notably larger than the sub-circular posterior facet of the more posterior element. The latter appears convex, although this is likely due to abrasion of the facet's rim.

The parapophyses are large, subtriangular and located anterodorsally on the lateral surfaces of the centra. They are asymmetrical in the anterior element, with the right parapophysis seemingly larger and more prominent. On the posterior centrum, the parapophyses appear less developed, although it seems likely they have been substantially weathered. The floors of the intervertebral foramina are visible bilaterally as wide and posteroventrally trending channels present on the dorsal surface of the more posterior centrum.

The dorsolateral surfaces, ventral to the neurocentral junction, are variably indented. The right lateral depression on the anterior centrum is best developed, in contrast to its far shallower counterpart, whilst those on the posterior centrum are more similar in development. These depressions do not house pneumatic foramina, and their poor development indicates these are unlikely to pertain to a pneumatic system.

The ventral margins are only shallowly concave in lateral view. The ventral surface of the anterior centrum is rounded in transverse section along its length. Similar rounding is present on the posterior centrum; however, this element goes on to develop a shallow midline sulcus posteriorly. This sulcus is associated with a degree of mediolateral expansion of the bone, with the latter centrum thus appearing posteriorly wider relative to the equivalent end of the anterior element when viewed ventrally.

The relative position of the sacral vertebrae is difficult to determine given their incompleteness. The plesiomorphic dinosaurian (and archosaurian) sacrum consisted of two “primordial vertebrae” (Langer & Benton 2006; Moro et al. 2021). This count increased to five in tetanurans via the addition of dorso- and caudosacrals (Holtz et al. 2004). The primordial sacral vertebrae are thought to fuse prior to the evolutionarily ‘younger’ elements (O'Connor 2007), suggesting that IWCMS 2018.30.2 may represent this pair in the absence of a completely fused series. However, recognition of sacral fusion patterns in theropods remain complicated (Moro et al. 2021) and the identification of primordial sacrals is largely based on their sacral ribs and associated attachment points on the ilium (Nesbitt 2009), neither of which can be assessed here.

IWCMS 2018.30.3 (Anterior caudal vertebra)

A large partial caudal vertebra preserves only its posterior portion, having suffered a transverse shear posterior to the prezygapophyses (Fig. 6). It is among the most complete and informative of the elements known for this dinosaur. Fine cracks are apparent across the external bone surfaces, most notably affecting the centra. Both transverse processes and the neural spine have been lost, whilst abrasion to the postzygapophyses and margins of various neural arch laminae is apparent. Minor crushing appears to affect the left side of the element, as evidenced by the flattening of the ipsilateral rim of the posterior articular facet in posterior view. The left portion of said facet also appears abraded such that the underlying trabecular bone is exposed; abrasion also affects the rim of the right half of the facet. Metric data are presented in Table 3.

In life, the centrum was tall relative to its width (Fig. 6A), with the dorsoventral midline height of the posterior facet appearing unaffected by the crushing experienced along its left lateral side. The lateral margins are concave in coronal section, as is the ventral margin in lateral view. It is difficult to determine whether the neurocentral suture is closed: in places, the suture looks highlighted by specks of a black mineral (which also dots many of the abraded surfaces and cracks throughout the element), but it is unclear if this represents retention of the open state or is a taphonomic artefact. The broken anterior surface does not preserve obvious evidence of internal pneumatic features such as camerae or camellae (Britt 1993; Britt 1997) (Fig. 6B). The distinction between the cortical and cancellous bone is obvious in places, with the former measuring 4.8mm on the left ventrolateral side; it appears to thin dorsally towards the neurocentral suture. The cross-section of the infilled neural canal is visible in anterior view. It is largely circular, but its mid-ventral margin bulges ventrally.

The ventral surface of the centrum is heavily distorted. Although no keel is present, crushing on the left side has distorted the surface and its original shape can only be supposed; based on the better-preserved right side, it was likely largely convex in transverse section (Fig. 6C).

The lateral surfaces of the centrum present an elongate pleurocentral depression dorsally. On the better-preserved right side, a trifecta of small and presumably vascular foramina penetrate the right lateral surface. The dorsal two are smaller and located along the anterior and posterior ventral margins of the pleurocentral depression, with the larger, more ventral foramen positioned in line with the latter. Posteriorly, the mid-dorsal rim of the tall and moderately concave posterior articular facet is shallowly indented, above which sits the inversely ovate neural canal.

The neural arch is robust, with thick walls made visible in the anterior cross-section. It preserves various fossae, some of which are delimited by stout laminae and may bilaterally vary in shape (Fig. 6D–F). Along the anterodorsal midline, the spinoprezygapophyseal fossa is deepest posteriorly and narrows mediolaterally towards the neural spine, being bordered by variably developed laminae; the right lamina is sharper than the contralateral structure. The dorsal rim of the former is more complete, preserving a dorsally curving anterior portion where it rose to meet the ipsilateral prezygapophyseal pedicle in lateral view.

Prezygocentrodiapophyseal and centrodiapophyseal fossae excavate the lateral neural arch surfaces. The former are deep and possess a largely triangular outline via two constraining lamina: the largely horizontal prezygodiapophyseal lamina forms its dorsal border, while the notably thick and obliquely oriented anterior centrodiapophyseal lamina delimits the fossa ventrally. The latter also forms the anterior margin of the bilaterally asymmetrical centrodiapophyseal fossae. The left is more developed, excavating the neural arch ventral to the transverse process to a deeper extent; the right, fossa, in contrast, is hardly perceptible. Posteriorly, the posterior centrodiapophyseal lamina forms a thick buttress to the transverse process. Postzygocentrodiapophyseal fossae are absent in this element.

The neural spine is posteriorly positioned on the neural arch. The base of the spine is mediolaterally thin and anteroposteriorly short and is webbed via variably developed spinodiapophyseal sulci and ridges (Fig. 6F, G). The postzygapophyses are insufficiently preserved at their posterior ends to warrant useful description, although the dorsoventrally tall spinopostygapophyseal fossa they enclosed is narrow and slit-like. No obvious hyposphene is present ventral to the remnants of the postzygapophyses (indeed, there appears to be no space between the spinopostzygapophyseal fossa and dorsal margin of the neural canal in which one could be present), although a small mass of cemented bone and sandstone overhangs the neural canal posteriorly.

The positioning of IWCMS 2018.30.3 within the caudal series derives from multiple lines of evidence. Indeed, several more anterior axial positions can be readily excluded. The dorsal positions of the transverse processes and their buttressing laminae eliminate most of the cervical series from consideration. In addition, the absence of a ventral keel is inconsistent with the condition present in posterior cervicals and anterior dorsals. The absence of internal pneumaticity within the centrum also indicates a more posterior position given that pneumatisation of the cervical and anterior dorsal centra is the "common pattern" amongst theropods (Benson et al. 2012). The lack of sacral ribs or their facets excludes a sacral position. Finally, the ovate shape of the posterior articular facet resembles the condition present in theropod posterior dorsal and anterior caudal vertebrae (Rauhut 2003), as does the presence of spinodiapophyseal webbing (observed in such elements in spinosaurid taxa especially).

We consider it most likely that IWCMS 2018.30.3 represents an anterior caudal vertebra, rather than the mid- or posterior dorsal vertebra for several reasons: a hyposphene, postzygocentrodiapophyseal fossae and accessory centrodiapophyseal laminae are all absent, and the neural spine is anteroposteriorly short. Hyposphenes are typical of dorsal vertebrae in large saurischians (although they can occur in the posterior cervical and anterior caudal vertebrae too) (Langer 2004; Rauhut 2003; Stefanic & Nesbitt 2019), and are present in the mid- and posterior dorsal vertebrae of *Baryonyx* (NHMUK PV R9951) (Charig & Milner 1997), IWCMS 2012.563 (Hutt & Newbery 2004), *Suchomimus* (MNN GDF 500) and *Ichthyovenator* (MDS BK 10-01) (Allain et al. 2012) where they are ventral to a broad spinopostzygapophyseal fossa and separate the latter from the neural canal. Hyposphene-free anterior caudal vertebrae are common amongst spinosaurids (Barker et al. 2021): a hyposphene is present in the putative anterior caudal neural arch of *Baryonyx* (Charig & Milner 1997) but – as discussed above – the identification of this element as an anterior caudal vertebrae may be an error. The absence of a hyposphene means that the spinopostzygapophyseal fossa is located dorsal to the neural canal (as seen in IWCMS 2018.30.3). The fossae concerned may also be narrower than their equivalents in the dorsal vertebrae, as noted in the anterior caudal vertebrae of *Riparovenator* (Barker et al. 2021) and *Vallibonavenatrix* (Malafaia et al. 2020b), although we concede that the narrow condition present in IWCMS 2018.30.3 may be exaggerated by loss of its postzygapophyses.

The pair of centrodiapophyseal fossae in IWCMS 2018.30.3 also differs from the three present in the mid and posterior dorsal vertebrae of such spinosaurids as *Baryonyx* (Charig & Milner 1997), *Ichthyovenator* (Allain et al. 2012), *Vallibonavenatrix* (Malafaia et al. 2020b), *Spinosaurus* (Stromer 1915) and *Suchomimus* (MNN GDF 500). Some of these taxa present an accessory centrodiapophyseal lamina in this vicinity, a trait typically recovered as synapomorphic of Baryonychinae but also present in the phylogenetically labile taxon *Ichthyovenator* (Allain et al. 2012; Barker et al. 2021; Benson 2010; Carrano et al. 2012; Holtz et al. 2004; Rauhut & Pol 2019). Given the absence to date of spinosaurine spinosaurids (see also below) in the Wealden

Supergroup, an accessory lamina might be expected if this element were a mid- or posterior dorsal vertebra.

The lack of a chevron facet – a characteristic feature of caudal vertebrae – would appear to count against a caudal identification for IWCMS 2018.30.3. However, chevron facets are absent on the anteriormost caudal centra of some tetanurans (Holtz et al. 2004). Further support for a caudal identification is provided by the anteroposteriorly short and posteriorly positioned neural spine, the position and anatomy of which recalls the condition in the anterior caudal vertebrae of *Riparovenator* (Barker et al. 2021) (see also Table 4). Caudal vertebrae of basal tetanurans may be amphicoelous or amphiplatyan (Holtz et al. 2004), and the concave posterior facet of IWCMS 2018.30.3 recalls the amphicoelous anatomy of *Ichthyovenator* (Allain et al. 2012), the spinosaurine FSAC-KK 11888 (Ibrahim et al. 2020a) and *Vallibonavenatrix* (Malafaia et al. 2020b).

IWCMS 2018.30.4 (Sacrocaudal fragment)

The damaged and fragmentary vertebra (Fig. 7A–D) was also recovered; it lacks many of its original margins and its dorsal surface is obscured by matrix. Useful morphometric data is difficult to obtain in light of its preservation. Its asymmetry presumably represents a degree of plastic deformation. The anterior and posterior surfaces have been damaged, although one surface (perhaps the posterior one, see below) appears to preserve a degree of bevelling in its ventral part, though this may be taphonomic in origin. The fragment possesses a width of 68.1 mm (measured across the ventral midpoint), a maximum height of 70.6 mm, and a maximum length of 74.6 mm. The most noteworthy osteological feature pertains to a prominent and wide anteroposteriorly oriented sulcus on its ventral surface.

The longitudinal ventral sulcus of IWCMS 2018.30.4 suggests that this fragment might be an incomplete caudal centrum. Ventral sulci are common on theropod caudal vertebrae including those of spinosaurids (Samathi *et al.* 2021), although we note that Rauhut (2003) did not observe any in the cf. *Suchomimus* caudal element MNN GDF 510. The somewhat bevelled ventral portion of the posterior surface may be a chevron facet. Additionally, the fragment is similar in ventral view to anterior caudal vertebrae of *Vallibonavenatrix* (Malafaia *et al.* (2020b): Fig 6E). However, we cannot exclude the possibility that IWCMS 2018.30.4 is a sacral vertebra: it is similar to the other sacral elements in width, and the presence of a ventral sulcus is a feature seen in spinosaurid sacral vertebrae, including those of *Vallibonavenatrix* (Malafaia et al. 2020b) and possibly *Camarillasaurus* (Samathi et al. 2021).

IWCMS 2018.30.5 and 6 (Rib fragments)

A pair of rib shaft fragments are preserved (Fig. 7E–J), although it cannot be determined whether they pertain to the same element. The larger one, which is associated with a confused mess of bone fragments cemented to its surfaces, has a length of 194.0 mm. The other measures 144.3

mm and is largely well preserved despite the loss of its dorsal and ventral segments. A triangular cross-section with rounded corners is apparent in the latter, the widest of the three surfaces measuring 80.8 mm. Whilst this morphology was likely present ventrally in the larger piece (despite the damage sustained to one of the margins), this fragment appears to flare and flatten dorsally, suggesting that it originated near the rib head. The internal cross-section of the smaller fragment is infilled with cancellous bone. Such internal organisation could not be reliably ascertained via macroscopic examination of the larger fragment's extremities.

Appendicular elements

IWCMS 2018.30.7 and 8 (Rib fragments)

A pair of fragments representing a single, postacetabular process of a right-sided ilium were recovered. The fragments are poorly preserved and do not fit back together, though it would appear that only a slither of material is missing (Fig. 8). The fragments are large and robustly built, and lack any evidence of pneumaticity.

The remains of the brevis fossa can be distinguished, preserved as at least two separate pieces; the anterior piece measures ~135 mm (anteroposterior length), and the more posterior fragment ~145 mm. The medial side has been mostly stripped of its overlying cortical bone. The dorsally projecting postacetabular blade is missing, and what remains are medial and lateral blades that together enclose the brevis fossa. The former is incomplete and its extent difficult to assess, although it likely faced mainly ventrally. Enough of the ventrolaterally projecting lateral blade is well preserved to describe its generally thick and rounded morphology, posteriorly increasing ventrolateral projection, and flattened lateral surface. While stout anteriorly (with a dorsoventral thickness of 41.9 mm), it appears to thin posteriorly (dorsoventral height: 21.9 mm) before thickening again (dorsoventral height: 34.1 mm). When viewed ventrally, both pieces describe a posteriorly expanding fossa. A small neurovascular foramen is present on the anterior margin of the more anterior piece.

Additional fragments probably pertain to the ilium given their triradiate and triangular cross-section, but are very poorly preserved. These are briefly reported in the supplementary information.

IWCMS 2018.30.9 and 10 (Long bone fragments)

Two transverse slices of a long bone are preserved (Fig. 9), one with a largely sub-circular cross-section while the other likely possessed a more ovate cross-section in life. Both are damaged and offer little of note bar their diameter (107.8 mm and 123.7 mm respectively) and asymmetrical cortical bone thickness. The space enclosed by the cortical bone is occupied by cancellous bone with no evidence of a medullary cavity, perhaps suggesting the pieces derived from the metaphyseal region of the limb bone. It is uncertain as to whether both belong to the same element, and to which element that may be, although we presume it originates from the pelvic limb given the rest of the material recovered for this individual.

Systematic palaeontology

DINOSAURIA (Owen 1842)
THEROPODA (Marsh 1881)
TETANURAE (Gauthier 1986)
SPINOSAURIDAE (Stromer 1915)

Spinosauridae indet.

Referred specimens: IWCMS 2018.30 (Figs. 3–9), which includes a probable yet fragmentary anterior dorsal vertebra (2018.30.1), a pair of fused sacral centra (2018.30.2), a partial caudal vertebra (2018.30.3), a sacrocaudal centrum fragment (2018.30.4), rib fragments (2018.30.5, 6), pieces of ilium (2018.30.7, 8) and portions of long bone (2018.30.9, 10). Several other indeterminate fragments are also known (Fig. 10; see also supplementary information).
Locality and Horizon: White Rock Sandstone equivalent, Compton Chine, Vectis Formation (late Barremian).

Remarks

Phylogenetic results

The recovery the White Rock spinosaurid as an early branching member of Spinosaurinae within our agreement subtree (Fig. 3B) is intriguing, especially considering the current absence of the clade from Lower Cretaceous deposits of the British Isles. Spinosaurines may have originated in Europe (Barker et al. 2021), and phylogenetic and quantitative analyses of fragmentary materials support their presence in the quasi-contemporaneous deposits of Iberia (Alonso & Canudo 2016; Alonso et al. 2018; Isasmendi et al. 2020; Malafaia et al. 2020a; Sánchez-Hernández et al. 2007). The three above-listed spinosaurine synapomorphies were also recovered in the previous iteration of the analysis used here (Barker et al. 2021).

However, the distribution of these three caudal character states could potentially be a function of the relative position of these elements along the axial column. Indeed, specimens such as FSAC-KK 11888 (Ibrahim et al. 2020a) and MN 4743-V (Bittencourt & Kellner 2004) appear to show that fossae and laminae become less prominent in the more posterior parts of the axial skeleton. We consider IWCMS 2018.30.3 to be more anteriorly placed than any of the known caudal elements of *Riparovenator* or *Vallibonavenatrix* (specimens that are also known from anterior caudal material); scores regarding fossae or laminae for the latter pair's anterior caudal series might thus be affected by a lack of positional overlap. Comparisons are exacerbated by our incomplete knowledge of the anteriormost caudal series of other relevant taxa, such as *Baryonyx* and *Suchomimus* (Charig & Milner 1997; Sereno et al. 1998). In addition, the presence of centrodiapophyseal (Ch. 358:1) and prezygodiapophyseal laminae (Ch. 626:1) is [illegible] unique to Spinosaurinae: rather, these character states are homoplastic amongst tetanurans.

Importantly, Jackknife resampling does not lend support to a spinosaurine affinity for the White Rock spinosaurid, placing it within a polytomy alongside both spinosaurine and baryonychine taxa (Fig. 3C). Our understanding of character distribution within spinosaurid tails would very obviously benefit from the discovery of more complete (i.e. overlapping) anterior caudal vertebrae from non-spinosaurine taxa, and we do not consider the recovered synapomorphies to be sufficiently diagnostic to warrant referral of the White Rock spinosaurid to Spinosaurinae at this time.

Further comparisons

The presence of a sub-parapophyseal sulcus in the probable dorsal vertebra IWCMS 2018.30.1 is similar to the (albeit better developed) sulci described in the anterior dorsal centrum of the indeterminate tetanuran *Vectaerovenator* (Barker et al. 2020). Similarly positioned sulci are present in the possible megalosauroid *Yunyangosaurus* (Dai et al. 2020). While *Vectaerovenator*'s incomplete nature requires that its phylogenetic position remains ambiguous, it is interesting that constrained phylogenetic analyses found that few extra steps were required to recover it within Megalosauroidea (Barker et al. 2020) and it possesses at least some features (including enlarged pneumatic foramina) akin to the synapomorphic condition of megalosaurian anterior dorsal centra (Carrano et al. 2012). However, caution is advised when discussing this character in IWCMS 2018.30.1, given the state of preservation on the contralateral side that precludes assessment of any mirroring.

The possible presence of a median tuberosity in IWCMS 2018.30.1 is similar to that observed in the posterior cervical and anterior dorsals of *Sigilmassasaurus* (Evers et al. 2015), and would suggest the feature is more broadly distributed amongst spinosaurids. The robust ventral keel differs from theropods more generally, with anterior dorsal centra in particular typically producing deep, sharp keels (Rauhut 2003). However, robust keels may occur around the cervicodorsal region and are perhaps a function of overall s[illegible] given the tendency for increased keel robusticity in larger elements of some spinosaurid material (Evers et al. 2015).

The shallowly concave, nearly horizontal lateral profile of the ventral margins of the sacral vertebrae (IWCMS 2018.30.2) is typical of many theropods. They lack the strongly arched condition of various ceratosaurs (Carrano et al. 2012; Carrano & Sampson 2008; Rauhut & Pol 2019). The anteroposteriorly elongate centra are similar to those of other spinosaurids including *Suchomimus*, *Vallibonavenatrix* and *Camarillasaurus*, although such dimensions also occur in some ceratosaurs and *Megalosaurus* (Samathi et al. 2021). The presence of a ventral sulcus on the posterior sacral centrum recalls a similar structure on the third sacral of *Vallibonaventrix* (Malafaia et al. 2020b) but it does not extend as far anteriorly in the White Rock spinosaurid. The sacral centra also recalls *Vallibonaventrix* and the lost *Spinosaurus aegyptiacus* type specimen (Stromer 1915) in possessing depressed lateral surfaces. So called "pleurocentral depressions" have been deemed synapomorphic for Allosauria and Megalosauridae in some analyses (Carrano et al. 2012; Rauhut & Pol 2019), but are also present in various coelurosaurs (Holtz et al. 2004), with those of IWCMS 2018.30.2 poorly developed compared to such taxa as *Megalosaurus* (Benson 2010) and *Allosaurus* (Gilmore 1920). As above, we consider the features in IWCMS 2018.30.2 to represent non-pneumatic lateral indentations; the centra thus remain apneumatic, as is typical of non-avian theropods but contrasts with the condition in *Vallibonavenatrix* (Malafaia et al. 2020b).

The anteroposteriorly narrow neural spine (relative to neural arch length) of IWCMS 2018.30.3 differs from longer condition observed in the "pelvic" axial series (i.e. the vertebral series encompassing the posterior dorsals to the anterior caudals) of such spinosaurids as *Baryonyx* (Charig & Milner 1997), *Ichthyovenator* (Allain et al. 2012) and *Suchomimus* (the latter only preserves large, sheet-like neural spine tips in its anterior caudal series; Sereno *et al.* (1998): Fig. 3). When caudal elements are compared (Table 4), IWCMS 2018.30.3 is closest to *Riparovenator*, although (as mentioned previously) we consider the anteriormost preserved caudal element of the latter to occupy a comparatively more posterior position. Indeed, IWCMS 2018.30.3 differs from *Riparovenator* in the absence of an anterior spur (=accessory neural spine of some) at the base of the neural spine. Anterior spurs are more common towards the mid-caudal series in taxa presenting with the feature (Rauhut 2003), and are similarly absent from the anteriormost elements of *Ichthyovenator* (Allain et al. 2012) and the entirety of the caudal series of FSAC-KK 11888 (Ibrahim et al. 2020a).

Additionally, the lack of postzygocentrodiapophyseal fossae in IWCMS 2018.30.3 suggests a difference in centrodiapophyseal fossae morphology in this individual relative to some other spinosaurids. Three centrodiapophyseal fossae are present in the neural arches of the anterior caudal vertebrae of such specimens as the spinosaurine FSAC-KK 11888 (Ibrahim et al. 2020a), MN 4743-V (Bittencourt & Kellner 2004), the 'Phuwiang spinosaurid B' material (SMPW9B-14, 15) and probably *Ichthyovenator* (Samathi et al. 2021). However, as noted above, more convincing comparison can only take place when better corroboration pertaining to the proposed axial position of IWCMS 2018.30.3 occurs. Elsewhere on IWCMS 2018.30.3, the presence of pleurocentral depressions is also shared with the anterior caudal vertebrae of *Vallibonavenatrix* (Malafaia et al. 2020b) and *Iberospinus* (Mateus & Estraviz-López 2022).

The posteriorly diverging margins of the brevis fossa (IWCMS 2018.30.7, 8) recall the condition in *Baryonyx* (Charig & Milner 1997) and *Vallibonaventarix* (Malafaia et al. 2020b); indeed, this character state has previously been suggested as a synapomorphy of Baryonychinae *sensu* Barker *et al.* (2021). In *Ichthyovenator*, a taxon recovered in Barker *et al.* (2021) as a spinosaurine but whose affinities may not be as clear cut (Evers et al. 2015), the fossa is narrow and with subparallel margins (Allain et al. 2012). Posterior expansion of the brevis fossa is nevertheless common to Neotheropoda (Carrano et al. 2012) and is present in a variety of tetanurans (Benson 2010), indicating a wider distribution of the character state.

Brief biostratinomic comments

All elements that make up the specimens described here are highly fragmented. The transverse slices of long bone show variation in cortical thickness, perhaps exacerbated by varying degrees of delamination. Other elements display cracked, crazed and irregular surface markings. The best-preserved bones – the fused sacral vertebral centra (Fig. 5) – show longitudinal cracking, while some other bored elements (see below; Fig. 10) possess reasonably preserved cortex on one surface but roughened, irregular looking cortical surfaces elsewhere. These changes equate to stages 1-3 in Behrensmeyer's (1978) scale of weathering and abrasion, suggesting a possible pre-burial interval of 3-4 years. Given the highly fragmentary state, we note that trampling may also have occurred (Britt et al. 2009), and perhaps accounts for the crushed in left lateral surface of IWCMS 2018.30.3 in particular.

Bioerosion, represented by curved tubes of uniform width, is present on several elements and is interpreted as representing invertebrate feeding traces (Fig. 10A–G). These extend into the cancellous bone for ~80 mm and have circular cross-sections with a diameter of ~10 mm. Terrestrial bone borings with equivalent diameters have been recorded in the Upper Jurassic and throughout the Cretaceous (Britt et al. 2008; Csiki 2006; Paik 2000; Rogers 1992). In all cases, beetles (Coleoptera) were considered the most likely bioeroders. No bioglyphs are visible on our specimen, although the boring infills have been left in situ. When reassembled, the more medially placed circular cross-section in Fig. 10G abuts the marginally placed end of the longitudinal section of its counterpart in 10F, indicating the possibility of a right-angled branch or direction change. The borings were infilled by matrix and macroscopic bone chippings or frass are absent. This suggests that burial occurred after the bioerosion occurred.
Britt et al. (2008) considered borings more than 5 mm in depth to be ethologically indicative of internal mining or harvesting of bone. Necrophagous coleopterans and their larvae (in particular desmestids) are among the most common invertebrate bone modifiers (Xing et al. 2013) and feed on desiccated carcasses that are subaerially exposed (Bader et al. 2009; Cruzado-Caballero et al. 2021); osteophagy occurs when other food sources are exhausted (Bader et al. 2009), bone borings being more typically related to pupation (Höpner & Bertling 2017). Regardless, bioerosion created by dermestid-type beetles can involve the creation of tunnel (=tube)-like structures (Britt et al. 2008; Cruzado-Caballero et al. 2021; Höpner & Bertling 2017).

Circumstantial support for the possible importance of dermestids as bone modifiers in Wealden environments is provided by the existence of this group in the Middle Jurassic (Deng *et al.* 2017) and the fact that beetles are the most abundant of Wealden Supergroup insect, the caveat here being that they are mostly represented by elytra (which are mostly non-diagnostic to family level; Jarzembowski 2011).

Several other necrophagous insect groups can be excluded from consideration (Bader et al. 2009; Cruzado-Caballero et al. 2021; Xing et al. 2013): hymenopterans and isopterans typically produce star-shaped features and isopterans tend to cause more widespread, irregular damage, rather than tunnels (Hutchet 2014); tineid moths (Lepidoptera) specialise in keratinous tissues and traces made by them have yet to be identified in the fossil record; and the burrows of mayfly (Ephemeroptera) larvae are typically narrow, U-shaped, thin walled, and limited to aquatic environments anyway. Damage by other aquatic organisms such as burrowing bivalves are also improbable given the taphonomic circumstances and the curved form of the structures (such molluscs usually produce clavate-shaped borings; McHugh *et al.,* 2020), whilst the parallel-sided morphology with lack of splitting makes plant root damage unlikely (Rogers 1992).

An additional trace can be observed on the abraded medial surface of a fragment of ilium. It takes the form of a straight, wide, parallel-sided ‘furrow’ running that extends across the exposed cancellous bone (Fig. 8A) (at mid-length, some of the furrow’s margins have seemingly been eroded). As furrows typically describe open excavations affecting cortical bone (Britt et al. 2008; Pirrone et al. 2014), this structure might represent one side of a tube akin to those described above. Additional divot-like impressions are present on other pieces of the ilium, but these are difficult to separate from non-biological damage and are not considered further here. Elsewhere, several tooth mark-like traces are observed on the smaller rib fragment. However, they likely do not represent vertebrate feeding traces (D. Hone, pers. comms. 2021).
In sum, we tentatively attribute the traces to coleopteran bioerosion related to harvesting behaviour, but note that additional study is required.

Discussion

The presence of multiple theropod – and specifically spinosaurid – characters across various elements, combined with the consistency in size and preservation of the specimens, supports their referral to a single spinosaurid individual. Given the state of preservation of the material, classification to a more precise taxonomic rank is currently not possible, and the specimen is best classified as Spinosauridae indet. The White Rock spinosaurid likely does represent a new taxon, but we are unable to diagnose it based on the material to hand.

The discovery of this specimen in the basal unit of the Vectis Formation renders it the youngest documented spinosaurid material from the Wealden Supergroup. Previous finds from the Wealden Group had been restricted to the underlying Wessex Formation (Barker et al. 2021; Hutt & Newbery 2004; Martill & Hutt 1996) and no spinosaurid material is known from equivalent outcrops in Dorset (Penn et al. 2020). A possible contemporary is perhaps represented be a worn tooth crown (NHMUK PV R 5165, initially referred to *Goniopholis crassidens*) recovered from Atherfield on the Isle of Wight (Fowler 2007), a locality that contains outcrops of the Vectis Formation. Unfortunately, precise stratigraphic information is missing for this specimen.

Comparisons with the spinosaurid record from the younger members of the neighbouring Weald Clay Group are more difficult. The Upper Weald Clay Formation yielded the type specimen of *Baryonyx walkeri* (Charig & Milner 1986) and is largely synchronous with the exposed Wealden Group strata on the Isle of Wight. The base of this formation is Barremian in age, but its upper age has proven difficult to constrain and may be late Barremian or early Aptian (Radley & Allen 2012b); indeed, the palynomorph, ostracod and mollusc faunas of the upper units of the Upper Weald Clay Formation are similar to those of the Vectis Formation (Radley & Allen 2012b). However, the *Baryonyx walkeri* type specimen was recovered from Smokejacks Pit in Ockley, Surrey, whose exposures in the Upper Weald Clay Formation are consistent with an early Barremian age (Radley & Allen 2012b; Ross & Cook 1995). A baryonychine tooth crown (MNEMG 1996.133) was recovered from Ewhurst's Brickworks (Surrey) from a layer equivalent to the top of the Smokejacks beds (Charig & Milner 1997). We are unaware of any younger spinosaurid occurrences from the Weald Clay Group, although the historical nature of many accessioned Wealden specimens renders it difficult to collate precise stratigraphic information. Nevertheless, spinosaurids are known from the late Barremian and early Aptian of Iberia (Malafaia et al. 2020a), suggesting the potential existence of younger British specimens.

Despite the general rarity of Vectis Formation dinosaur remains, ichnological evidence from the White Rock Sandstone suggests the sandflat facies supported large dinosaur populations that visited the fluctuating, plant colonised shoreline (Radley & Allen 2012c; Radley et al. 1998). More generally, the recovery of spinosaurid remains from this formation is perhaps expected. Not only are its units within the temporal span of the clade, spinosaurid remains from lagoonal deposits have been documented elsewhere (see Bertin (2010) for a review of depositional environments containing spinosaurid remains), and their occurrences have been shown to correlate with 'coastal' palaeoenvironments (relative to other sampled taxa) (Sales et al. 2016), a broad category that includes paralic environments (Butler & Barrett 2008).

A remarkable feature of the White Rock spinosaurid is its large size (Table 5). Large theropods from the underlying Wessex Formation include the allosauroid *Neovenator salerii* (Brusatte et al. 2008; Hutt et al. 1996) and the spinosaurids *Ceratosuchops* and *Riparovenator* (Barker et al. 2021). While ichnological evidence reinforces the presence of particularly large forms in the Wessex Formation (Lockwood 2016), the Vectis Formation spinosaurid appears to eclipse the above taxa in size as well as other European theropods.

The fragmentary megalosaurine caudal vertebra MUJA-1913 is currently regarded as the largest European theropod skeletal material (based on the dorsoventral height of its posterior articular facet). Its size suggests an individual more than 10m in length (Rauhut et al. 2018). A set of large caudal vertebrae from the Oxfordian (Jurassic) of France with potential megalosaurid affinities are said to be of comparable size, but have yet to be published in detail (Pharisat 1993; Rauhut et al. 2018). IWCMS 2018.30.3 exceeds the dorsoventral proportions of MUJA-1913 (Table 5). Similarly, the anterior sacral vertebra of the White Rock spinosaurid is larger anteroposteriorly (~156 mm) than that of spinosaurids for which data is known, including *Vallibonavenatrix* (five recovered vertebrae, length range: 90–96 mm) (Malafaia et al. 2020b) and FSAC KK-11888 (three vertebrae, length range: 135–145 mm) (Ibrahim et al. 2014), being sub-equal to the largest sacral element of the *Spinosaurus* type specimen (of three vertebrae, lengths for the two most complete ones are >130 mm–155 mm) (Stromer 1915). The brevis fossa in IWCMS 2018.30.7 also supports these extrapolations: the maximum measurable width is 84.6 mm but the fossa probably flared to a greater width when complete. In comparison, the fossa has a maximum width of ~50 mm in *Ichthyovenator* (based on Allain *et al*. 2012: Fig. S7), 60 mm in *Vallibonavenatrix* (Malafaia et al. 2020b), and ~70 mm in *Allosaurus* (based on Madsen, 1976, pl. 46B).

Aureliano *et al.* (2018) suggested that the evolution of large body sizes (i.e. 10–15 m) in Spinosaurinae may be linked to their semi-aquatic specialisations; indeed, selection for increased size has been noted amongst aquatic vertebrates in general (Gearty et al. 2018; Heim et al. 2015). However, the definition of ‘semi-aquatic’ remains problematic within the context of spinosaurid ecology; not only is aquatic adaptation within spinosaurines a disputed issue (Hone & Holtz Jr 2019), there is also the fact that the apparently less aquatic baryonychines (Arden et al. 2019; Hone & Holtz Jr 2021) also exceeded 10 m (Sereno et al. 1998; Therrien & Henderson 2007). At the time of writing the degree and nature of aquatic adaptations within spinosaurids remains the topic of research (Barker et al. 2017; Henderson 2018; Hone & Holtz Jr 2019; Hone & Holtz Jr 2021); nevertheless, it is not clear that giant size in Spinosaurinae is linked to aquatic habits. The discovery of the large-bodied White Rock spinosaurid, lacking unambiguous spinosaurine affinities or traits suggestive of enhanced aquatic specialisation (e.g. increased bone density), lends some support to this contention.

In sum, whilst the precariousness of extrapolating overall body size from singular bones and dimensions cannot be understated, the impressive proportions of the White Rock spinosaurid material (IWCMS 2018.30.3 in particular) demonstrate the presence of a notably large tetanuran in the Wealden Supergroup of Britain: one that rivalled or even exceeded the largest theropods recovered elsewhere from the European Mesozoic.

Conclusions

The White Rock spinosaurid represents the first documented spinosaurid from the Vectis Formation of the Isle of Wight, extending the temporal span of the clade in the British fossil record to the late Barremian. This stratigraphic positioning also renders it the youngest spinosaurid known the UK. The White Rock spinosaurid is likely a novel taxon, however the specimen lacks convincing autapomorphies and we instead refer this specimen to Spinosauridae indet. Our phylogenetic analysis was unable to resolve its position within Spinosauridae, however weakly supported spinosaurine or early-branching spinosaurid affinities were recovered in some data runs for this specimen. Though fragmentary, it is the largest theropod currently known from the Wealden Supergroup, with some metrics exceeding those of the largest theropods known from Europe more generally.

Acknowledgements

We thank Serjoscha Evers and Steve Hutt for useful comments regarding spinosaurid vertebral anatomy; Dave Hone for thoughts on vertebrate feeding traces; Steve Vidovich for advice on phylogenetics; Phil James (ilium and long bone fragments) and Mick Green (axial elements) for their expert preparation of the material; and Mark Penn for kindly donating a vertebral fragment. Additional thanks are extended to Mick Green, who kindly prepared elements gratis. The program TNT is made available thanks to the Willi Hennig Society. This study was supported by the Engineering and Physical Sciences Research Council (EPSRC), UK and the Institute for Life Sciences, University of Southampton, UK.

Institutional Abbreviations

FSAC, Faculté des Sciences, Casablanca University, Casablanca, Morocco;
IWCMS, Isle of Wight County Museum Services, Dinosaur Isle Museum, Isle of Wight, UK;
MDS, Dinosaur Museum, Savannahket, Laos;
MNEMG. Maidstone Museum, Kent, UK;
MN, Museu Nacional, Rio de Janeiro, Brazil;
MNBN, Musée National Boubou Hama, Niamey, Niger;
MNN, Musée National du Niger, Niamey, Niger;
MSM, Museo Paleontológico Juan Cano Forner, Sant Mateu, Castellón, Spain;
MUJA, Museo del Jurásico de Asturias, Colunga, Spain;
NHMUK, Natural History Museum, London, UK;
SM, Sirindhorn Museum, Department of Mineral Resources, Kalasin, Thailand.

References

Allain R, Xaisanavong T, Richir P, and Khentavong B. 2012. The first definitive Asian spinosaurid (Dinosauria: Theropoda) from the early cretaceous of Laos. *Naturwissenschaften* 99:369-377.

Alonso A, and Canudo JI. 2016. On the spinosaurid theropod teeth from the early Barremian (Early Cretaceous) Blesa Formation (Spain). *Historical Biology* 28:823-834.
Alonso A, Gasca J, Navarro-Lorbés P, Rubio C, and Canudo J. 2018. A new contribution to our knowledge of the large-bodied theropods from the Barremian of the Iberian Peninsula: the “Barranco del Hocino” site (Spain). *Journal of Iberian Geology* 44:7-23.
Amiot R, Buffetaut E, Lécuyer C, Fernandez V, Fourel F, Martineau F, and Suteethorn V. 2009. Oxygen isotope composition of continental vertebrate apatites from Mesozoic formations of Thailand; environmental and ecological significance. *Geological Society, London, Special Publications* 315:271-283.
Amiot R, Buffetaut E, Lécuyer C, Wang X, Boudad L, Ding Z, Fourel F, Hutt S, Martineau F, and Medeiros MA. 2010. Oxygen isotope evidence for semi-aquatic habits among spinosaurid theropods. *Geology* 38:139-142.
Arden TMS, Klein CG, Zouhri S, and Longrich NR. 2019. Aquatic adaptation in the skull of carnivorous dinosaurs (Theropoda:Spinosauridae) and the evolution of aquatic habits in spinosaurids. *Cretaceous Research* 93:275-284. 10.1016/j.cretres.2018.06.013
Aureliano T, Ghilardi AM, Buck PV, Fabbri M, Samathi A, Delcourt R, Fernandes MA, and Sander M. 2018. Semi-aquatic adaptations in a spinosaur from the Lower Cretaceous of Brazil. *Cretaceous Research* 90:283-295.
Austen PA, and Batten DJ. 2018. English Wealden fossils: an update. *Proceedings of the Geologists' Association* 129:171-201.
Bader KS, Hasiotis ST, and Martin LD. 2009. Application of forensic science techniques to trace fossils on dinosaur bones from a quarry in the Upper Jurassic Morrison Formation, northeastern Wyoming. *Palaios* 24:140-158.
Barker CT, Hone DW, Naish D, Cau A, Lockwood JA, Foster B, Clarkin CE, Schneider P, and Gostling NJ. 2021. New spinosaurids from the Wessex Formation (Early Cretaceous, UK) and the European origins of Spinosauridae. *Scientific Reports* 11:1-15.
Barker CT, Naish D, Clarkin CE, Farrell P, Hullmann G, Lockyer J, Schneider P, Ward RK, and Gostling NJ. 2020. A highly pneumatic middle Cretaceous theropod from the British Lower Greensand. *Papers in Palaeontology*.
Barker CT, Naish D, Newham E, Katsamenis OL, and Dyke G. 2017. Complex neuroanatomy in the rostrum of the Isle of Wight theropod *Neovenator salerii*. *Scientific Reports* 7:3749. 10.1038/s41598-017-03671-3
Batten DJ. 2011. Wealden Geology. In: Batten DJ, ed. *English Wealden Fossils*. London: The Palaeontological Association, 7-14.
Behrensmeyer AK. 1978. Taphonomic and ecologic information from bone weathering. *Paleobiology* 4:150-162.
Benson RB. 2010. A description of *Megalosaurus bucklandii* (Dinosauria: Theropoda) from the Bathonian of the UK and the relationships of Middle Jurassic theropods. *Zoological Journal of the Linnean Society* 158:882-935.
Benson RB, Butler RJ, Carrano MT, and O'Connor PM. 2012. Air-filled postcranial bones in theropod dinosaurs: physiological implications and the ‘reptile’–bird transition. *Biological Reviews* 87:168-193.
Benton MJ, and Spencer PS. 1995. *Fossil reptiles of Great Britain*. Dordrecht: Springer.
Bertin T. 2010. A catalogue of material and review of the Spinosauridae. *PalArch’s Journal of Vertebrate Palaeontology* 7:1-39.
Bittencourt J, and Kellner AWA. 2004. On a sequence of sacrocaudal theropod dinosaur vertebrae from the Lower Cretaceous Santana Formation, northeastern Brazil. *Arq Mus Nac* 62:309-320.
Blows WT. 1987. The armoured dinosaur *Polacanthus foxi* from the Lower Cretaceous of the Isle of Wight. *Palaeontology* 30:557-580.

Britt BB. 1993. Pneumatic cranial bones in dinosaurs and other archosaurs. PhD. University of Calgary.

Britt BB. 1997. Postcranial pneumaticity. In: Currie PJ, and Padian K, eds. *The Encyclopedia of Dinosaurs*. San Diego: Academic Press, 590-593.

Britt BB, Eberth DA, Scheetz RD, Greenhalgh BW, and Stadtman KL. 2009. Taphonomy of debris-flow hosted dinosaur bonebeds at Dalton Wells, Utah (Lower Cretaceous, Cedar Mountain Formation, USA). *Palaeogeography, Palaeoclimatology, Palaeoecology* 280:1-22.

Britt BB, Scheetz RD, and Dangerfield A. 2008. A suite of dermestid beetle traces on dinosaur bone from the Upper Jurassic Morrison Formation, Wyoming, USA. *Ichnos* 15:59-71.

Brusatte SL, Benson RBJ, and Hutt S. 2008. *The osteology of Neovenator salerii (Dinosauria: Theropoda) from the Wealden Group (Barremian) of the Isle of Wight*. London: Monograph of the Palaeontographical Society.

Buffetaut E. 2010. Spinosaurs before Stromer: early finds of spinosaurid dinosaurs and their interpretations. In: Moody RTJ, Buffetaut E, Naish D, and Martill DM, eds. *Dinosaurs and Other Extinct Saurians: A Historical Perspective*: The Geological Society of London, 175–188.

Butler RJ, and Barrett PM. 2008. Palaeoenvironmental controls on the distribution of Cretaceous herbivorous dinosaurs. *Naturwissenschaften* 95:1027-1032.

Carrano MT, Benson RB, and Sampson SD. 2012. The phylogeny of Tetanurae (Dinosauria: Theropoda). *Journal of Systematic Palaeontology* 10:211–300.

Carrano MT, and Sampson SD. 2008. The phylogeny of ceratosauria (Dinosauria: Theropoda). *Journal of Systematic Palaeontology* 6:183-236.

Cau A. 2018. The assembly of the avian body plan: a 160-million-year long process. *Bollettino della Società Paleontologica Italiana* 57:1-25.

Charig AJ, and Milner AC. 1986. *Baryonyx*, a remarkable new theropod dinosaur. *Nature* 324:359-361.

Charig AJ, and Milner AC. 1997. *Baryonyx walkeri*, a fish-eating dinosaur from the Wealden of Surrey. *Bulletin-Natural History Museum Geology Series* 53:11-70.

Coria RA, and Currie PJ. 2016. A new megaraptoran dinosaur (Dinosauria, Theropoda, Megaraptoridae) from the Late Cretaceous of Patagonia. *PLOS ONE* 11.

Cruzado-Caballero P, Canudo JI, De Valais S, Frigola J, Barriuso E, and Fortuny J. 2021. Bioerosion and palaeoecological association of osteophagous insects in the Maastrichtian dinosaur *Arenysaurus ardevoli*. *Lethaia*.

Csiki Z. 2006. Insect borings in dinosaur bone from the Maastrichtian of the Hateg Basin, Romania - paleoecological and paleoclimatic implications. 101-109. In: Csiki Z, ed. *Mesozoic and Cenozoic Vertebrates and Paleoenviroments Tributes to the career of Prof Dan Grigorescu*. Cambridge: Cambridge University Press, 95-104.

Dai H, Benson R, Hu X, Ma Q, Tan C, Li N, Xiao M, Hu H, Zhou Y, and Wei Z. 2020. A new possible megalosauroid theropod from the Middle Jurassic Xintiangou Formation of Chongqing, People's Republic of China and its implication for early tetanuran evolution. *Scientific Reports* 10:1-16.

Evers SW, Rauhut OW, Milner AC, McFeeters B, and Allain R. 2015. A reappraisal of the morphology and systematic position of the theropod dinosaur *Sigilmassasaurus* from the "middle" Cretaceous of Morocco. *PeerJ* 3:e1323.

Fowler D. 2007. Recently rediscovered baryonychine teeth (Dinosauria: Theropoda): New morphologic data, range extension & similarity to *Ceratosaurus*. *Journal of Vertebrate Paleontology* 27:76A-76A.

Gauthier J. 1986. Saurischian monophyly and the origin of birds. *Memoirs of the California Academy of sciences* 8:1-55.

Gearty W, McClain CR, and Payne JL. 2018. Energetic tradeoffs control the size distribution of aquatic mammals. *Proceedings of the National Academy of Sciences* 115:4194-4199.
Gilmore CW. 1920. Osteology of the carnivorous Dinosauria in the United States National museum: with special reference to the genera *Antrodemus* (*Allosaurus*) and *Ceratosaurus*. *Bulletin of the United States National Museum* i-xi:1-159.
Goloboff PA, and Catalano SA. 2016. TNT version 1.5, including a full implementation of phylogenetic morphometrics. *Cladistics* 32:221-238.
Hassler A, Martin J, Amiot R, Tacail T, Godet FA, Allain R, and Balter V. 2018. Calcium isotopes offer clues on resource partitioning among Cretaceous predatory dinosaurs. *Proceedings of the Royal Society B: Biological Sciences* 285:20180197.
Heim NA, Knope ML, Schaal EK, Wang SC, and Payne JL. 2015. Cope's rule in the evolution of marine animals. *Science* 347:867-870.
Henderson DM. 2018. A buoyancy, balance and stability challenge to the hypothesis of a semi-aquatic *Spinosaurus* Stromer, 1915 (Dinosauria: Theropoda). *PeerJ* 6:e5409.
Holtz TR, Molnar RE, and Currie PJ. 2004. Basal Tetanurae. In: Weishampel DB, Dodson P, and Osmólska H, eds. *The Dinosauria*: University of California Press, 71-110.
Hone D, Xu X, and Wang D. 2010. A probable baryonychine (Theropoda: Spinosauridae) tooth from the Upper Cretaceous of Henan Province, China. *Vertebrata PalAsiatica* 48:19–26.
Hone DWE, and Holtz Jr TR. 2017. A century of spinosaurs - a review and revision of the Spinosauridae with comments on their ecology. *Acta Geologica Sinica - English Edition* 91:1120-1132. 10.1111/1755-6724.13328
Hone DWE, and Holtz Jr TR. 2019. Comment on: Aquatic adaptation in the skull of carnivorous dinosaurs (Theropoda: Spinosauridae) and the evolution of aquatic habits in spinosaurids. 93: 275–284. *Cretaceous Research*:104152.
Hone DWE, and Holtz Jr TR. 2021. Evaluating the ecology of *Spinosaurus*: Shoreline generalist or aquatic pursuit specialist? *Palaeontologia Electronica* 23:a03.
Hooley RW. 1925. On the skeleton of *Iguanodon atherfieldensis* sp. nov., from the Wealden Shales of Atherfield (Isle of Wight). *Quarterly Journal of the Geological Society* 81:1-61.
Höpner S, and Bertling M. 2017. Holes in bones: ichnotaxonomy of bone borings. *Ichnos* 24:259-282.
Hutchinson JR. 2001. The evolution of pelvic osteology and soft tissues on the line to extant birds (Neornithes). *Zoological Journal of the Linnean Society* 131:123-168.
Hutt S, Martill DM, and Barker MJ. 1996. The first European allosaurid dinosaur (Lower Cretaceous, Wealden Group, England). *Neues Jahrbuch für Geologie und Paläontologie-Monatshefte*:635-644.
Hutt S, and Newbery P. 2004. An exceptional theropod vertebra from the Wessex Formation (Lower Cretaceous) Isle of Wight, England. *Proceedings of the Isle of Wight Natural History and Archaeological Society* 20:61-76.
Ibrahim N, Maganuco S, Dal Sasso C, Fabbri M, Auditore M, Bindellini G, Martill DM, Zouhri S, Mattarelli DA, and Unwin DM. 2020a. Tail-propelled aquatic locomotion in a theropod dinosaur. *Nature* 581:67-70.
Ibrahim N, Sereno PC, Dal Sasso C, Maganuco S, Fabbri M, Martill DM, Zouhri S, Myhrvold N, and Iurino DA. 2014. Semiaquatic adaptations in a giant predatory dinosaur. *Science* 345:1613-1616.
Ibrahim N, Sereno PC, Varricchio DJ, Martill DM, Dutheil DB, Unwin DM, Baidder L, Larsson HC, Zouhri S, and Kaoukaya A. 2020b. Geology and paleontology of the Upper Cretaceous Kem Kem Group of eastern Morocco. *ZooKeys* 928:1.
Insole AN, and Hutt S. 1994. The palaeoecology of the dinosaurs of the Wessex Formation (Wealden Group, Early Cretaceous), Isle of Wight, Southern England. *Zoological Journal of the Linnean Society* 112:197-215.

Isasmendi E, Sáez-Benito P, Torices A, Navarro-Lorbés P, and Pereda-Suberbiola X. 2020. New insights about theropod palaeobiodiversity in the Iberian Peninsula and Europe: Spinosaurid teeth (Theropoda, Megalosauroidea) from the Lower Cretaceous of La Rioja (Spain). *Cretaceous Research* 116:104600.

Kerth M, and Hailwood E. 1988. Magnetostratigraphy of the Lower Cretaceous Vectis Formation (Wealden Group) on the Isle of Wight, southern England. *Journal of the Geological Society* 145:351-360.

Langer MC. 2004. Basal Saurischia. In: Weishampel DB, Dodson P, and OsmÓLska H, eds. *The Dinosauria*. 2 ed: University of California Press, 25-46.

Langer MC, and Benton MJ. 2006. Early dinosaurs: a phylogenetic study. *Journal of Systematic Palaeontology* 4:309-358.

Lockwood J. 2016. Ichnological evidence for large predatory dinosaurs in the Wessex Formation (Wealden Group, Early Cretaceous) of the Isle of Wight. *Proceedings of the Isle of Wight Natural History and Archaeological Society* 30:103-110.

Lomax DR, and Tamura N. 2014. *Dinosaurs of the British Isles*: Siri Scientific Press Manchester.

Malafaia E, Gasulla J, Escaso F, Narvaéz I, and Ortega F. 2020a. An update of the spinosaurid (Dinosauria: Theropoda) fossil record from the Lower Cretaceous of the Iberian Peninsula: distribution, diversity, and evolutionary history. *Journal of Iberian Geology* 46:431-444.

Malafaia E, Gasulla JM, Escaso F, Narváez I, Sanz JL, and Ortega F. 2020b. A new spinosaurid theropod (Dinosauria: Megalosauroidea) from the upper Barremian of Vallibona, Spain: Implications for spinosaurid diversity in the Early Cretaceous of the Iberian Peninsula. *Cretaceous Research* 106:104221.

Marsh OC. 1881. Principal characters of American Jurassic dinosaurs, part V. *American Journal of Science*:417-423.

Martill DM, and Hutt S. 1996. Possible baryonychid dinosaur teeth from the Wessex Formation (Lower Cretaceous, Barremian) of the Isle of Wight, England. Proceedings of the Geologists' Association. p 81-84.

Martill DM, and Naish D. 2001a. Dinosaurs of the Isle of Wight. Palaeontological Association, London. p 433.

Martill DM, and Naish D. 2001b. The geology of the Isle of Wight. In: Martill DM, and Naish D, eds. *Dinosaurs of the Isle of Wight*. London: The Palaeontological Association, 25-43.

Mateus O, and Estraviz-López D. 2022. A new theropod dinosaur from the early cretaceous (Barremian) of Cabo Espichel, Portugal: Implications for spinosaurid evolution. *PLOS ONE* 17:e0262614.

McCurry MR, Evans AR, Fitzgerald EM, McHenry CR, Bevitt J, and Pyenson ND. 2019. The repeated evolution of dental apicobasal ridges in aquatic-feeding mammals and reptiles. *Biological Journal of the Linnean Society* 127:245-259.

McHugh JB, Drumheller SK, Riedel A, and Kane M. 2020. Decomposition of dinosaurian remains inferred by invertebrate traces on vertebrate bone reveal new insights into Late Jurassic ecology, decay, and climate in western Colorado. *PeerJ* 8:e9510.

Milner AC. 2003. Fish-eating theropods: a short review of the systematics, biology and palaeobiogeography. Actas de las II Jornadas Internacionales sobre Paleontología de Dinosaurios y su Entorno: Salas de los Infantes (Burgos, España), septiembre de 2001: Caja de Burgos. p 129-138.

Moro D, Kerber L, Müller RT, and Pretto FA. 2021. Sacral co-ossification in dinosaurs: The oldest record of fused sacral vertebrae in Dinosauria and the diversity of sacral co-ossification patterns in the group. *Journal of Anatomy* 238:828-844.

Naish D, Hutt S, and Martill DM. 2001. Saurischian dinosaurs 2: Theropods. . In: Martill DM, and Naish D, eds. *Dinosaurs of the Isle of Wight*. London: The Palaeontological Association 242-309.

Naish D, and Martill DM. 2007. Dinosaurs of Great Britain and the role of the Geological Society of London in their discovery: basal Dinosauria and Saurischia. *Journal of the Geological Society* 164:493–510.

Naish D, and Martill DM. 2008. Dinosaurs of Great Britain and the role of the Geological Society of London in their discovery: Ornithischia. *Journal of the Geological Society* 165:613-623.

Nesbitt SJ. 2009. *The early evolution of archosaurs: relationships and the origin of major clades*: Columbia University.

Norman DB. 2004. Basal iguanodontia. In: Weishampel DB, Dodson P, and Osmólska H, eds. *The Dinosauria*. Berkeley CA: University of California Press, 413-437.

Norman DB. 2011. Ornithopod dinosaurs. In: Batten DJ, ed. *English Wealden Fossils*. London: The Palaeontological Association, 407-475.

O'Connor PM. 2007. The postcranial axial skeleton of *Majungasaurus crenatissimus* (Theropoda: Abelisauridae) from the Late Cretaceous of Madagascar. *Journal of Vertebrate Paleontology* 27:127-163.

Owen R. 1842. Report on British Fossil Reptiles Part II. Reports of the meetings of the British Association for the Advancement of Science: R. and JE Taylor. p 61–204.

Paik IS. 2000. Bone chip-filled burrows associated with bored dinosaur bone in floodplain paleosols of the Cretaceous Hasandong Formation, Korea. *Palaeogeography, Palaeoclimatology, Palaeoecology* 157:213-225.

Penn SJ, Sweetman SC, Martill DM, and Coram RA. 2020. The Wessex Formation (Wealden Group, Lower Cretaceous) of Swanage Bay, southern England. *Proceedings of the Geologists' Association* 131:679-698.

Pharisat A. 1993. Vertèbres de dinosaure (Théropode) dans l'Oxfordien de Plaimbois-du-Miroir (Doubs). *Société d'Histoire Nat du Pays Montbéliard, Montbéliard, Bull* 1993:191-192.

Pirrone CA, Buatois LA, and Bromley RG. 2014. Ichnotaxobases for bioerosion trace fossils in bones. *Journal of Paleontology* 88:195-203.

Pol D, and Escapa IH. 2009. Unstable taxa in cladistic analysis: identification and the assessment of relevant characters. *Cladistics* 25:515-527.

Pond S, Lockley MG, Lockwood JA, Breithaupt BH, and Matthews NA. 2014. Tracking dinosaurs on the Isle of Wight: a review of tracks, sites, and current research. *Biological Journal of the Linnean Society* 113:737-757.

Radley JD, and Allen P. 2012a. The non-marine Lower Cretaceous Wealden strata of southern England. *Proceedings of the Geologists' Association* 123:235-244.

Radley JD, and Allen P. 2012b. The Wealden (non-marine Lower Cretaceous) of the Weald sub-basin, southern England. *Proceedings of the Geologists' Association* 123:245-318.

Radley JD, and Allen P. 2012c. The Wealden (non-marine Lower Cretaceous) of the Wessex Sub-basin, southern England. *Proceedings of the Geologists' Association* 123:319-373.

Radley JD, and Barker MJ. 1998. Stratigraphy, palaeontology and correlation of the Vectis Formation (Wealden Group, Lower Cretaceous) at Compton Bay, Isle of Wight, southern England. *Proceedings of the Geologists' Association* 109:187-195.

Radley JD, Barker MJ, and Harding IC. 1998. Palaeoenvironment and taphonomy of dinosaur tracks in the Vectis Formation (Lower Cretaceous) of the Wessex Sub-basin, southern England. *Cretaceous Research* 19:471-487.

Rauhut OW. 2003. *The Interrelationships and Evolution of Basal Theropod Dinosaurs*: Blackwell Publishing.

Rauhut OW, Pinuela L, Castanera D, García-Ramos J-C, and Cela IS. 2018. The largest European theropod dinosaurs: remains of a gigantic megalosaurid and giant theropod tracks from the Kimmeridgian of Asturias, Spain. *PeerJ* 6:e4963.

Rauhut OW, and Pol D. 2019. Probable basal allosauroid from the early Middle Jurassic Cañadón Asfalto Formation of Argentina highlights phylogenetic uncertainty in tetanuran theropod dinosaurs. *Scientific Reports* 9:1–9.

Robinson SA, and Hesselbo SP. 2004. Fossil-wood carbon-isotope stratigraphy of the non-marine Wealden Group (Lower Cretaceous, southern England). *Journal of the Geological Society* 161:133-145.

Rogers RR. 1992. Non-marine borings in dinosaur bones from the Upper Cretaceous Two Medicine Formation, northwestern Montana. *Journal of Vertebrate Paleontology* 12:528-531.

Ross AJ, and Cook E. 1995. The stratigraphy and palaeontology of the Upper Weald Clay (Barremian) at Smokejacks Brickworks, Ockley, Surrey, England. *Cretaceous Research* 16:705-716.

Sales MA, Lacerda MB, Horn BL, de Oliveira IA, and Schultz CL. 2016. The "χ" of the matter: Testing the relationship between paleoenvironments and three theropod Clades. *PLOS ONE* 11:e0147031.

Salisbury SW, and Naish D. 2011. Crocodilians. In: Batten DJ, ed. *English Wealden Fossils*. London: The Palaeontological Association, 305-369.

Samathi A, Sander PM, and Chanthasit P. 2021. A spinosaurid from Thailand (Sao Khua Formation, Early Cretaceous) and a reassessment of *Camarillasaurus cirugedae* from the Early Cretaceous of Spain. *Historical Biology*:1-15.

Sánchez-Hernández B, Benton MJ, and Naish D. 2007. Dinosaurs and other fossil vertebrates from the Late Jurassic and Early Cretaceous of the Galve area, NE Spain. *Palaeogeography, Palaeoclimatology, Palaeoecology* 249:180-215.

Sereno PC, Beck AL, Dutheil DB, Gado B, Larsson HC, Lyon GH, Marcot JD, Rauhut OW, Sadleir RW, and Sidor CA. 1998. A long-snouted predatory dinosaur from Africa and the evolution of spinosaurids. *Science* 282:1298-1302.

Stefanic CM, and Nesbitt SJ. 2019. The evolution and role of the hyposphene-hypantrum articulation in Archosauria: phylogeny, size and/or mechanics? *Royal Society Open Science* 6:190258.

Stromer E. 1915. Ergebnisse der Forschungsreisen Prof. E. Stromers in den Wüsten Ägyptens. II. Wirbeltierreste der Baharîje Stufe (unterstes Cenoman). 3. Das Original des Theropoden *Spinosaurus aegyptiacus* nov. gen., nov. spec. . *Abhandlungen der Königlich Bayerischen Akademie der Wissenschaften, Mathematisch-physikalische Klasse Abhandlung* 28.

Sweetman SC. 2011. The Wealden of the Isle of Wight. In: Batten DJ, ed. *English Wealden Fossils*. London: The Palaeontological Association, 52-78.

Therrien F, and Henderson DM. 2007. My theropod is bigger than yours… or not: estimating body size from skull length in theropods. *Journal of Vertebrate Paleontology* 27:108-115.

Turmine-Juhel P, Wilks R, Brockhurst D, Austen PA, Duffin CJ, and Benton MJ. 2019. Microvertebrates from the Wadhurst Clay Formation (Lower Cretaceous) of Ashdown Brickworks, East Sussex, UK. *Proceedings of the Geologists' Association* 130:752-769.

Upchurch P. 1995. The evolutionary history of sauropod dinosaurs. *Philosophical Transactions of the Royal Society of London Series B: Biological Sciences* 349:365-390.

Upchurch P, Barrett PM, and Dodson P. 2004. Sauropoda. In: Weishampel DB, Dodson P, and Osmólska H, eds. *The Dinosauria*: University of California Press, 259-322.

Upchurch P, Mannion PD, and Barrett PM. 2011. Sauropod Dinosaurs. In: Batten DJ, ed. *English Wealden Fossils*. London: The Palaeontological Association, 476-525.

Weishampel DB, Barrett P, Coria RA, Le Loeuff J, Xing XU, Xijin Z, Sahni A, Gomani EMP, and Noto CR. 2004. Dinosaur distribution. In: Weishampel DB, Dodson P, and Osmólska H, eds. *The Dinosauria*. London, England: University of California Press, 517-606.

White MA, Bell PR, Poropat SF, Pentland AH, Rigby SL, Cook AG, Sloan T, and Elliott DA. 2020. New theropod remains and implications for megaraptorid diversity in the Winton Formation (lower Upper Cretaceous), Queensland, Australia. *Royal Society Open Science* 7:191462.

White O. 1921. *A Short Account of the Geology of the Isle of Wight*. London: Memoirs of the Geological Survey.

Whitlock JA. 2011. A phylogenetic analysis of Diplodocoidea (Saurischia: Sauropoda). *Zoological Journal of the Linnean Society* 161:872-915.

Wilson JA. 2011. Anatomical terminology for the sacrum of sauropod dinosaurs. *Contributions from the Museum of Paleontology, University of Michigan* 32:59-69.

Wilson JA, Michael D, Ikejiri T, Moacdieh EM, and Whitlock JA. 2011. A nomenclature for vertebral fossae in sauropods and other saurischian dinosaurs. *PLOS ONE* 6.

Xing L, Roberts EM, Harris JD, Gingras MK, Ran H, Zhang J, Xu X, Burns ME, and Dong Z. 2013. Novel insect traces on a dinosaur skeleton from the Lower Jurassic Lufeng Formation of China. *Palaeogeography, Palaeoclimatology, Palaeoecology* 388:58-68.

Table 1(on next page)

Metric data for IWCMS 2018.30.1.

Asterisk denotes taphonomic damage. Measurements are in millimetres (mm).

Table 1: Metric data for IWCMS 2018.30.1. Asterisk denotes taphonomic damage. Measurements are in millimetres (mm).

Anteroposterior length of the centrum (between ventral rims)*	69.4
Dorsoventral midline height of the anterior articular facet*	75.3
Mediolateral width of the anterior articular facet*	99.2
Dorsoventral midline height of the posterior facet*	92.5
Mediolateral width of the posterior facet*	118.5
Dorsoventral height of the right parapophysis	27.8
Anteroposterior length of the right parapophysis	25.7
Mediolateral width of the neural canal	39.7

Table 2(on next page)

Metric data for IWCMS 2018.30.2.

Asterisk denotes taphonomic damage. Measurements are in millimetres (mm).

Table 2: Metric data for IWCMS 2018.30.2. Asterisk denotes taphonomic damage. Measurements are in millimetres (mm).

Maximum anteroposterior length of the conjoined centra	298
Anteroposterior length of anterior centrum	~156
Anteroposterior length of posterior centrum	~142
Dorsoventral midline height of the exposed anterior articular facet*	118.1
Mediolateral midline width of the exposed anterior articular facet*	126.2
Dorsoventral midline height of the exposed posterior facet*	107.9
Mediolateral width of the exposed posterior facet*	102.7
Mediolateral width of the neural canal	40.7

Table 3 (on next page)

Metric data for IWCMS 2018.30.3.

Asterisk denotes taphonomic damage. Measurements are in millimetres (mm).

Table 3: Metric data for IWCMS 2018.30.3. Asterisk denotes taphonomic damage. Measurements are in millimetres (mm).

Dorsoventral height of posterior articular facet	159.8
Mediolateral width of the posterior articular facet*	112.8
Anteroposterior depth of the concavity of the posterior articular facet*	25.3
Anteroposterior length of the preserved centrum (right side)	106.5
Dorsoventral height of the anterior neural canal	38.6
Mediolateral width of the anterior neural canal	29.5
Anteroposterior length of the base of the neural spine	49.6
Mediolateral width of the base of the neural spine	16.8

Table 4(on next page)

Size of the anterior caudal neural spine base (collected from the most anterior preserved caudal element) relative to their respective neural arch in select spinosaurids.

Note that data for key taxa (e.g. *Baryonyx* and *Suchomimus*) is missing due to preservation. Asterisk denotes minimum metric due to preservation. Where neural arch base lengths are unknown, centrum length is used (denoted by †). Data collected from Allain *et al.* (2012), Ibrahim et al. (2020a) and Samathi*et al.* (2021). *Riparovenator* and FSAC-KK 11888 calculated via images using the scale function in FIJI (Schindelin et al. 2012).

Table 4: Size of the anterior caudal neural spine base (collected from the most anterior preserved caudal element) relative to their respective neural arch in select spinosaurids. Note that data for key taxa (e.g. *Baryonyx* and *Suchomimus*) is missing due to preservation. Asterisk denotes minimum metric due to preservation. Where neural arch base lengths are unknown, centrum length is used (denoted by †). Data collected from Allain *et al.* (2012), Ibrahim et al. (2020a) and Samathi *et al.* (2021). *Riparovenator* and FSAC-KK 11888 calculated via images using the scale function in FIJI (Schindelin et al. 2012).

Specimen	Spinosauridae indet. (IWCMS 2018.30.3)	"Phuwiang spinosaurid B" (SM-PW9B-15)	*Riparovenator* (IWCMS 2020.447.3)	*Ichthyovenator* (MDS BK10-02)	Spinosaurinae indet. (FSAC-KK 11888)
Basal neural arch length (mm)	112.9*	69	~138	101†	~55
Basal neural spine length (mm)	49.6	53	~45	68	~101
Neural spine length:neural arch length	0.43*	0.77	0.33	0.67	0.54

Table 5(on next page)

Comparative dorsoventral heights (in millimetres) of the posterior articular facets of the caudal vertebrae of various tetanurans.

Where several caudal vertebrae are known, the largest is presented here. Note that only data for the anterior articular facet is available for the lost *Spinosaurus* holotype and FSAC KK-11888 (marked by an asterisk). Data collected from Stromer (1915); Dong *et al.* (1983); Charig & Milner (1997); Brochu (2003: fig. 59A); Allain *et al*. (2012); Hendrickx & Mateus (2014); Rauhut *et al.* (2018); Ibrahim *et al.*(2020a); Samathi *et al.* (2021) and Mateus & Estraviz-López (2022). Measurements for *Riparovenator* taken by CTB.

Table 5: Comparative dorsoventral heights (in millimetres) of the posterior articular facets of the caudal vertebrae of various tetanurans. Where several caudal vertebrae are known, the largest is presented here. Note that only data for the anterior articular facet is available for the lost *Spinosaurus* holotype and FSAC KK-11888 (marked by an asterisk). Data collected from Stromer (1915); Dong *et al.* (1983); Charig & Milner (1997); Brochu (2003): Fig. 59A); Allain *et al*. (2012); Hendrickx & Mateus (2014); Rauhut *et al.* (2018); Ibrahim *et al.* (2020a); Samathi *et al.* (2021) and Mateus & Estraviz-López (2022). Measurements for *Riparovenator* taken by CTB.

Spinosauridae								Other tetanurans				
Spinosauridae indet. (IWCMS 2018.30.3)	*Baryonyx* (NHMUK PV R9951)	*Riparovenator* (IWCMS 2020.447.7)	*Ichthyovenator* (MDS BK10-03)	*Spinosaurus* (BSP 1912 VII 19)	Spinosaurinae indet. (FSAC KK-11888)	Phuwiang spinosaurid B" (SM-PW-9B-17)	*Iberospinus* (ML 1190-15)	*Tyrannosaurus rex* (FMNH PR2081)	*Yangchuanosaurus "magnus"* (CV00216)	*Torvosaurus gurneyi* (ML 1100)	Megalosaurinae indet. (MUJA-1913)
159.8	110	125.6	128	135*	129*	88	100.7	~257	140	145	150

Figure 1

General geological context of the White Rock spinosaurid material.

(A) Schematic palaeogeographic map of the Wealden Supergroup, highlighting the Wessex and Weald sub-basins (from Barker *et al.*(2021), modified from Penn *et al.* (2020): Fig. 2). (B) Schematic stratigraphy of the Wealden Group on the Isle of Wight (modified from Radley and Allen (2012c): Fig. 6), with relevant strata highlighted. (C) Map of the Isle of Wight, highlighting the outcrops of the Vectis Fm. and location of the spinosaurid remains (modified from Ruffell (1988): Fig. 1).

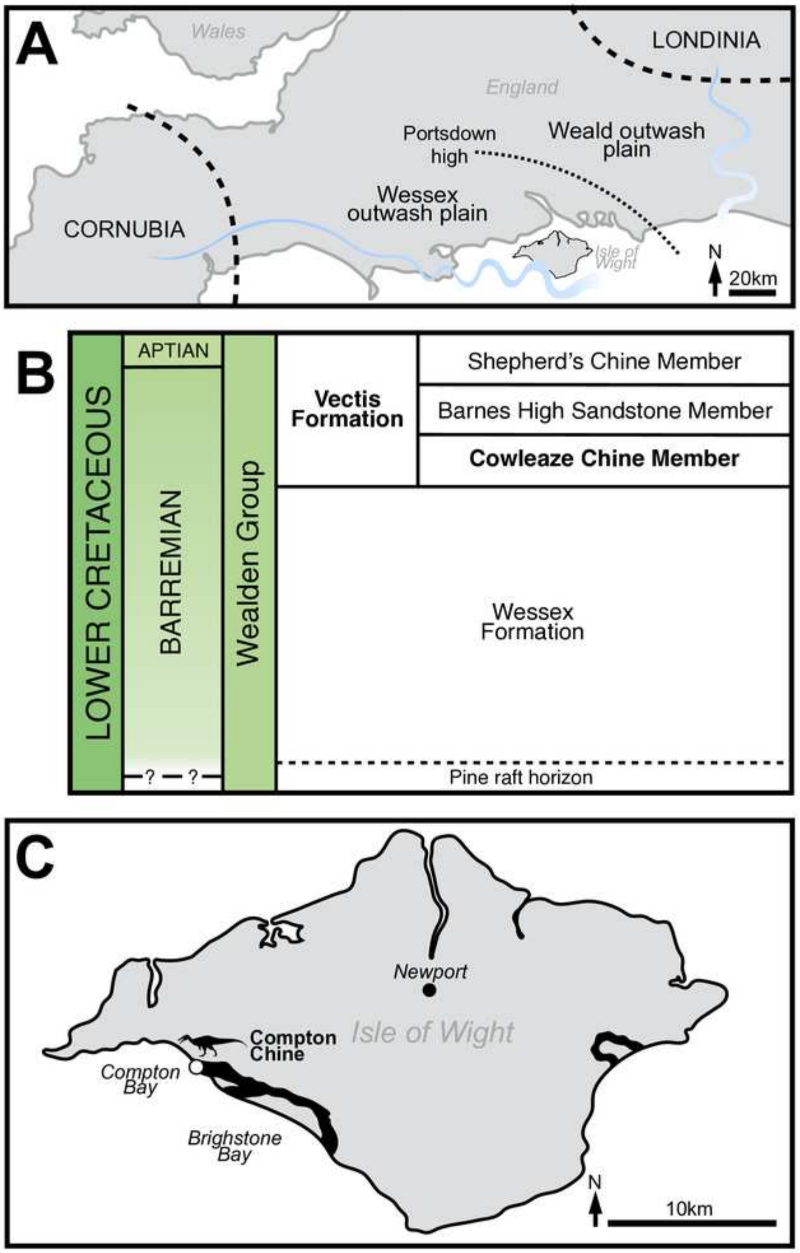
A
Wales
LONDINIA
England
Portsdown high
Weald outwash plain
Wessex outwash plain
CORNUBIA
Isle of Wight
N
20km
B
LOWER CRETACEOUS
APTIAN
BARREMIAN
Wealden Group
Vectis Formation
Shepherd's Chine Member
Barnes High Sandstone Member
Cowleaze Chine Member
Wessex Formation
Pine raft horizon
C
Newport
Compton Chine
Isle of Wight
Compton Bay
Brighstone Bay
N
10km

Figure 2

Stratigraphic context of the White Rock spinosaurid material.

(A) View of the cliff between Compton Chine and Shippards Chine (Compton Bay), highlighting the members of the Wealden Group and overlying Lower Greensand Group (from Radley & Barker, 1998: Fig. 2). (B) Junction between the Wessex and Vectis formations located towards Compton Chine. (C) Vertical section through the lower unit of the Vectis Formation, Compton Bay, Isle of Wight (modified from Radley & Allen (2012c): Fig. 26). Spinosaurid silhouette courtesy of Dan Folkes (CC-BY 4.0).

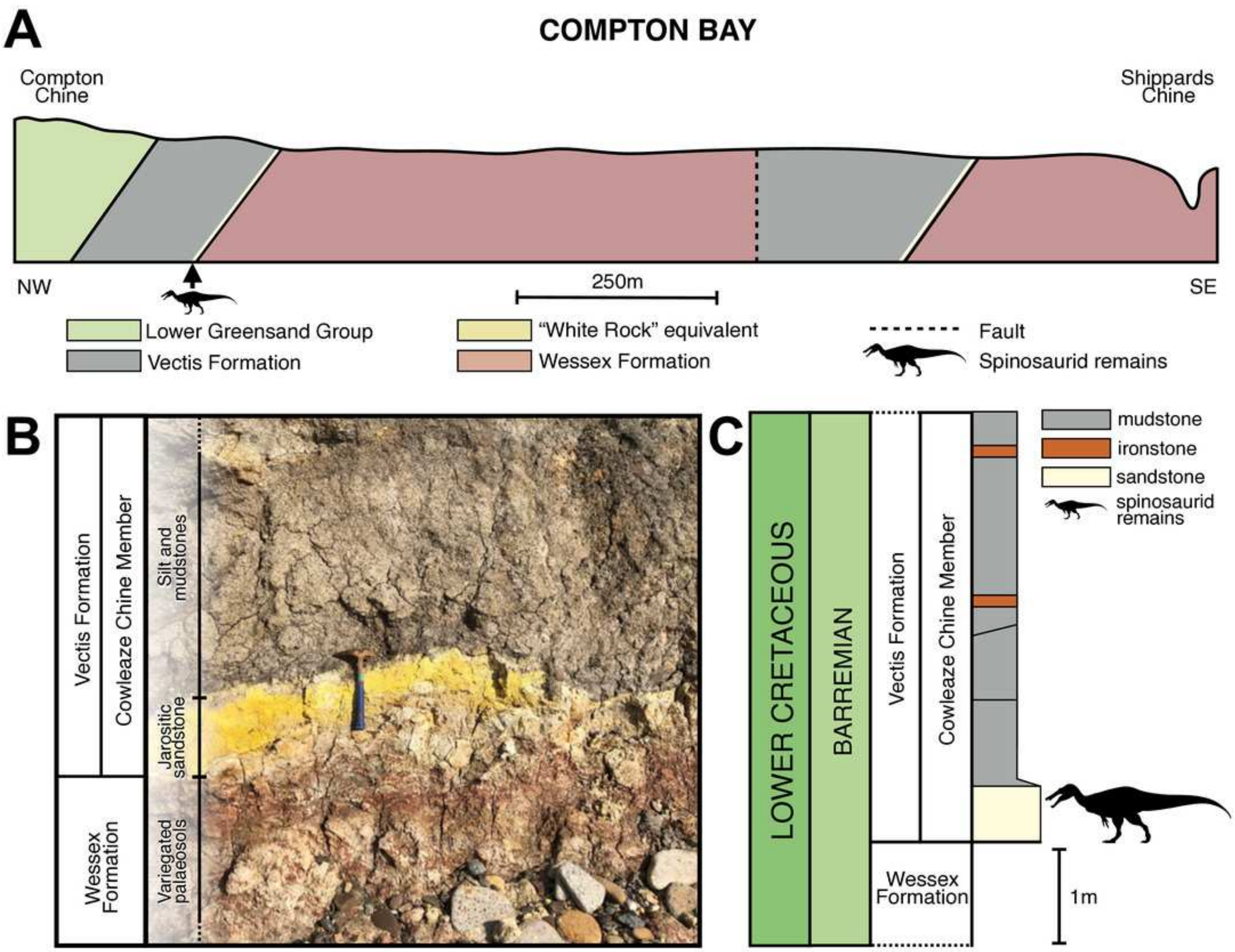
A
COMPTON BAY
Compton Chine
Shippards Chine
NW
SE
250m
Lower Greensand Group
Vectis Formation
"White Rock" equivalent
Wessex Formation
Fault
Spinosaurid remains
B
Vectis Formation
Cowleaze Chine Member
Wessex Formation
Silt and mudstones
Jarositic sandstone
Variegated palaeosols
C
LOWER CRETACEOUS
BARREMIAN
Vectis Formation
Cowleaze Chine Member
Wessex Formation
mudstone
ironstone
sandstone
spinosaurid remains
1m

Figure 3

Phylogenetic results following the addition of the White Rock spinosaurid to the modified dataset of Barker *et al.* (2021), focusing on Spinosauridae.

(A) Strict consensus tree (numbers above nodes indicate Bremer support values >1). (B) Maximum agreement subtree displaying stable spinosaurid taxa. (C) Jackknife resampling for nodal support (numbers below nodes indicate jackknife values above 50%). Full versions available in the supplementary information.

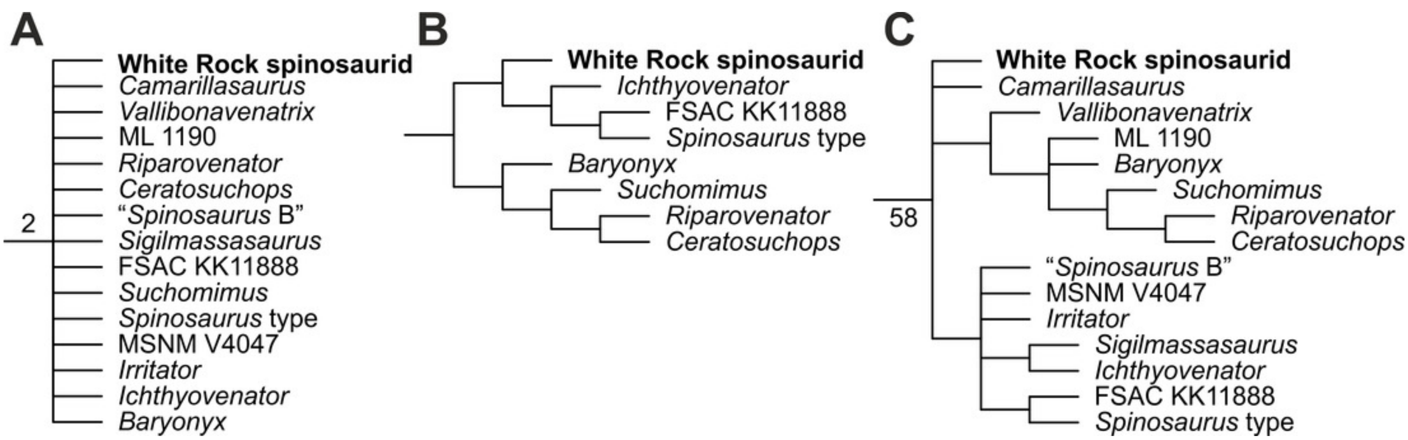

Figure 4

Probable anterior dorsal vertebral fragment IWCMS 2018.30.1.

(A) Right lateral view. (B) Left lateral view. (C) Anterior view. (D) Posterior view. (E) Dorsal view. F) Ventral view. *Abbreviations:*at, anterior tuberosity; k, keel; na, neural arch; nc, neural canal; pf, pneumatic foramen; pp, parapophysis; rim, flattened rim around the anterior articular facet; su, sulcus. Scale bar: 50 mm.

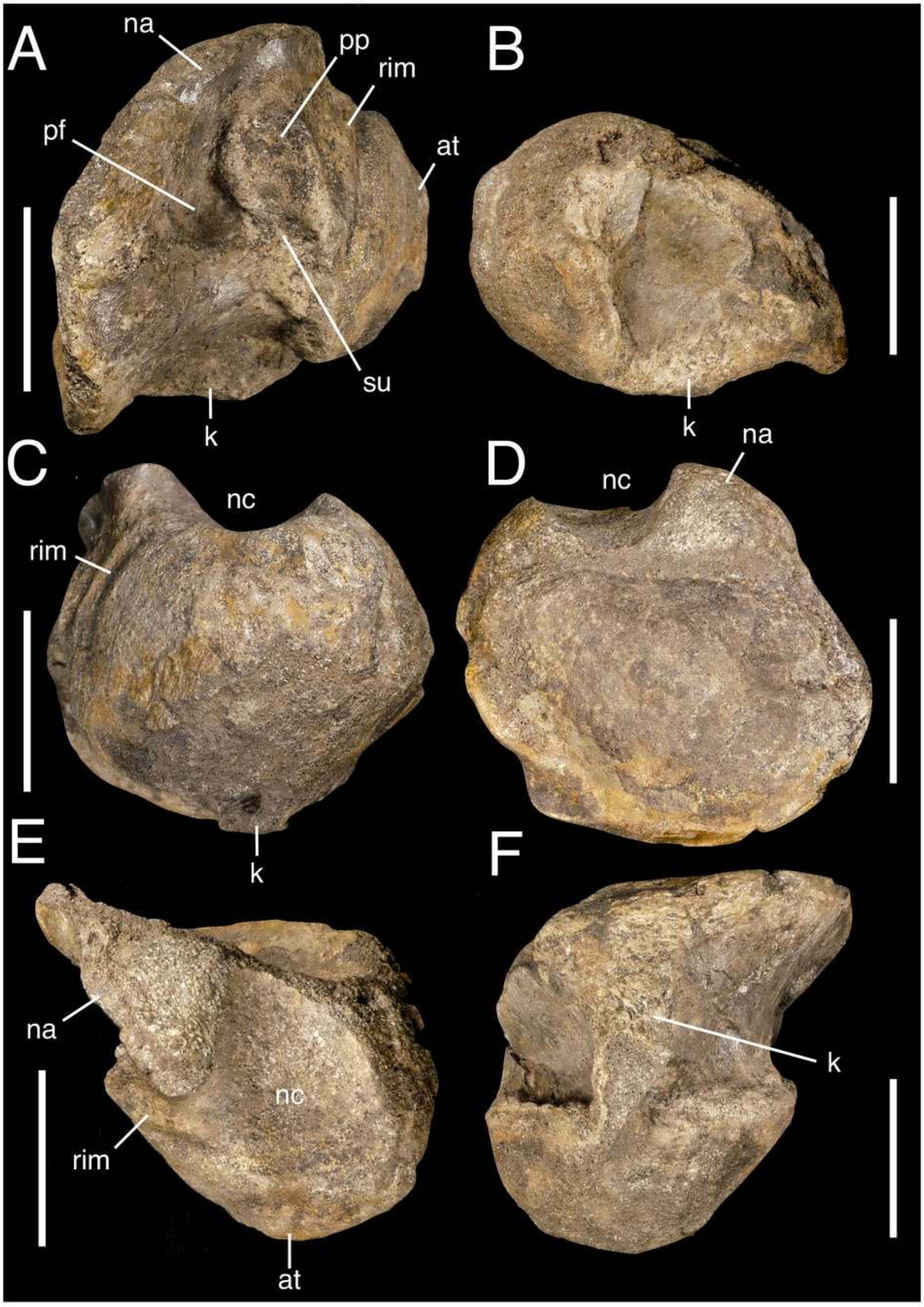
A
na
pp
rim
pf
at
su
k
B
k
C
nc
rim
k
D
nc
na
E
na
nc
rim
at
F
k

Figure 5

Conjoined sacral centra IWCMS 2018.30.2.

(A) Dorsal view. (B) Right lateral view. (C) Left lateral view. (D) Ventral view. (E) Anterior view. (F) Posterior view. *Abbreviations*: dep, depression; ivf, floor of the intervertebral foramen; nc, neural canal; pp, parapophysis; su, sulcus. Scale bars: 50 mm.

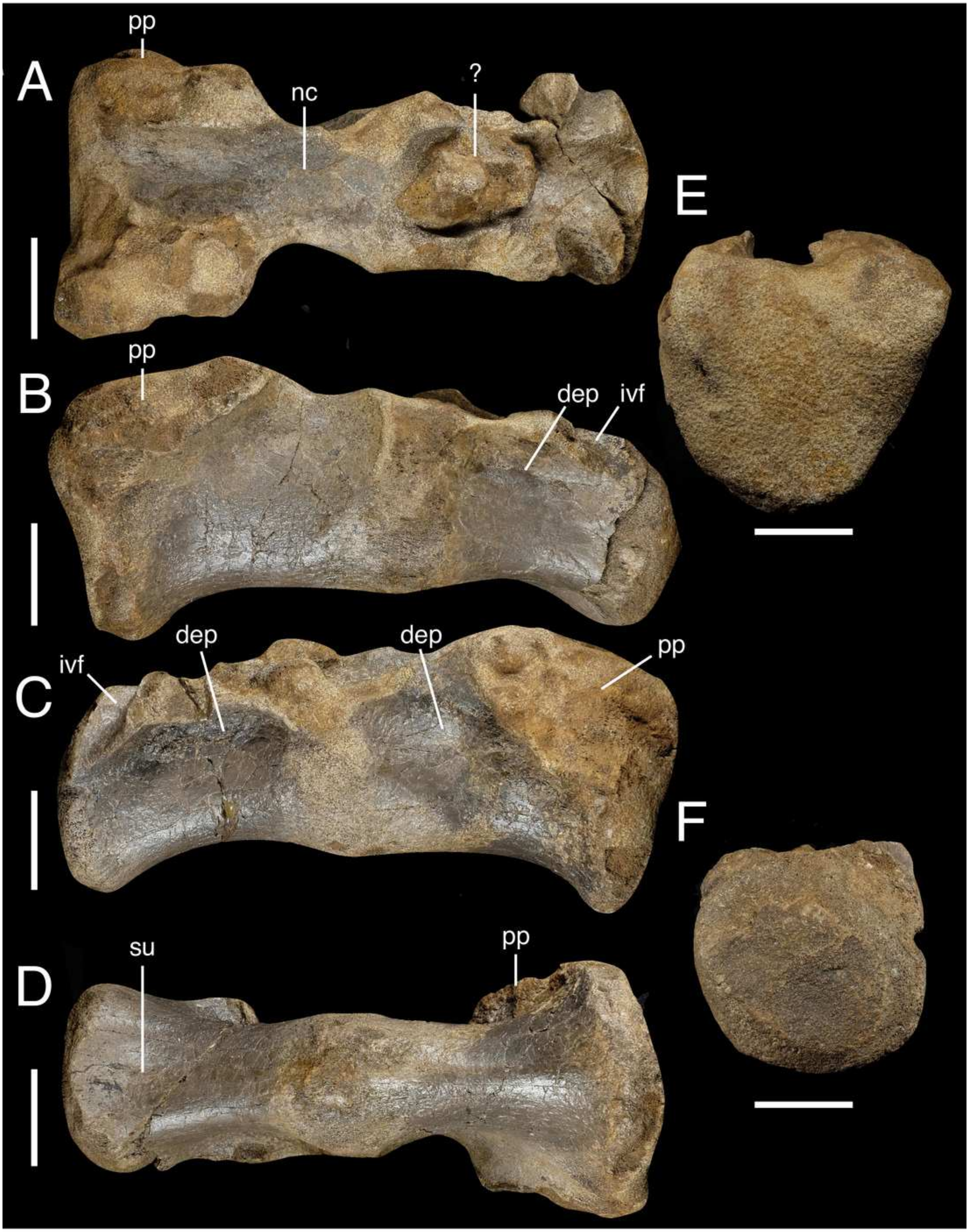
A
pp
nc
?
B
pp
dep
ivf
C
ivf
dep
dep
pp
D
su
pp
E
F

Figure 6

Partial caudal vertebra IWCMS 2018.30.3.

(A) Posterior view. (B) anterior view. (C) Ventral view. (D) Left lateral view. (E) Right lateral view. (F) dorsal view. (G) Right dorsolateral oblique view. *Abbreviations*: acdl, anterior centrodiapophyseal lamina; c, centrum; cdf, centrodiapophyseal fossa; nc, neural canal; ns, neural spine; pcd, pleurocentral depression; pcdl, posterior centrodiapophyseal lamina; prcdf, prezygocentrodiapophyseal fossa; sprf, spinoprezygapophyseal fossa; sprl, spinoprezygapophyseal lamina; spof, spinopostzygapophyseal fossa; web, spinodiapophyseal webbing. Scale bars: 50 mm.

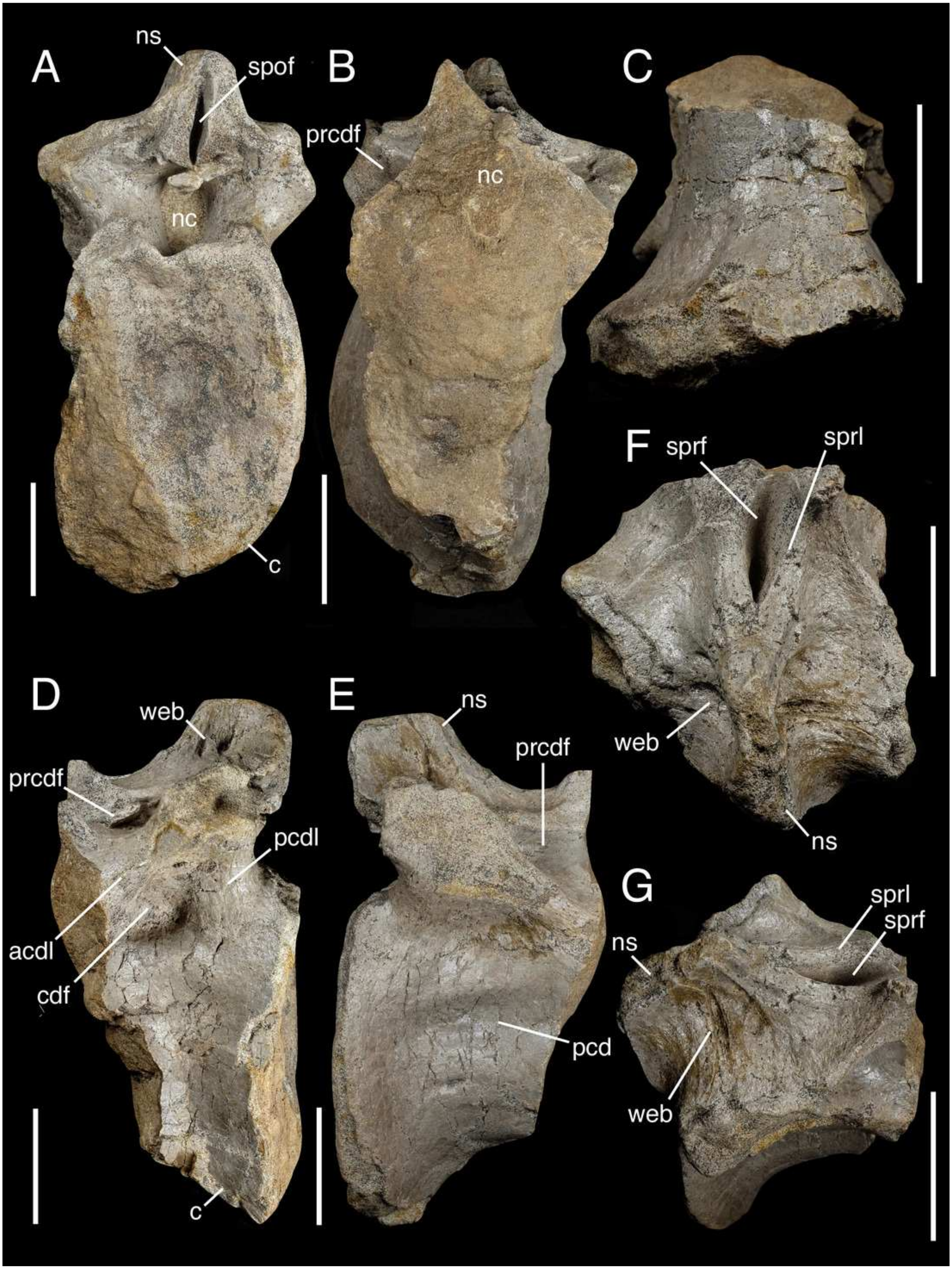
A
ns
spof
nc
c
B
prcdf
nc
C
D
web
prcdf
pcdl
acdl
cdf
c
E
ns
prcdf
pcd
F
sprf
sprl
web
ns
G
sprl
sprf
ns
web

Figure 7

Sacrocaudal fragment IWCMS 2018.30.4 (A–D) and rib fragments IWCMS 2018.30.5 (E–G) and 2018.30.6 (H–J).

(A) Dorsal view. (B) Posterior view. (C) Anterior view. (D) Ventral view. Views uncertain for IWCMS 2018.30.5 and 2018.30.6. *Abbreviations:* su: sulcus. Scale bars: 20 mm (A–G, J); 50 mm (H–I).

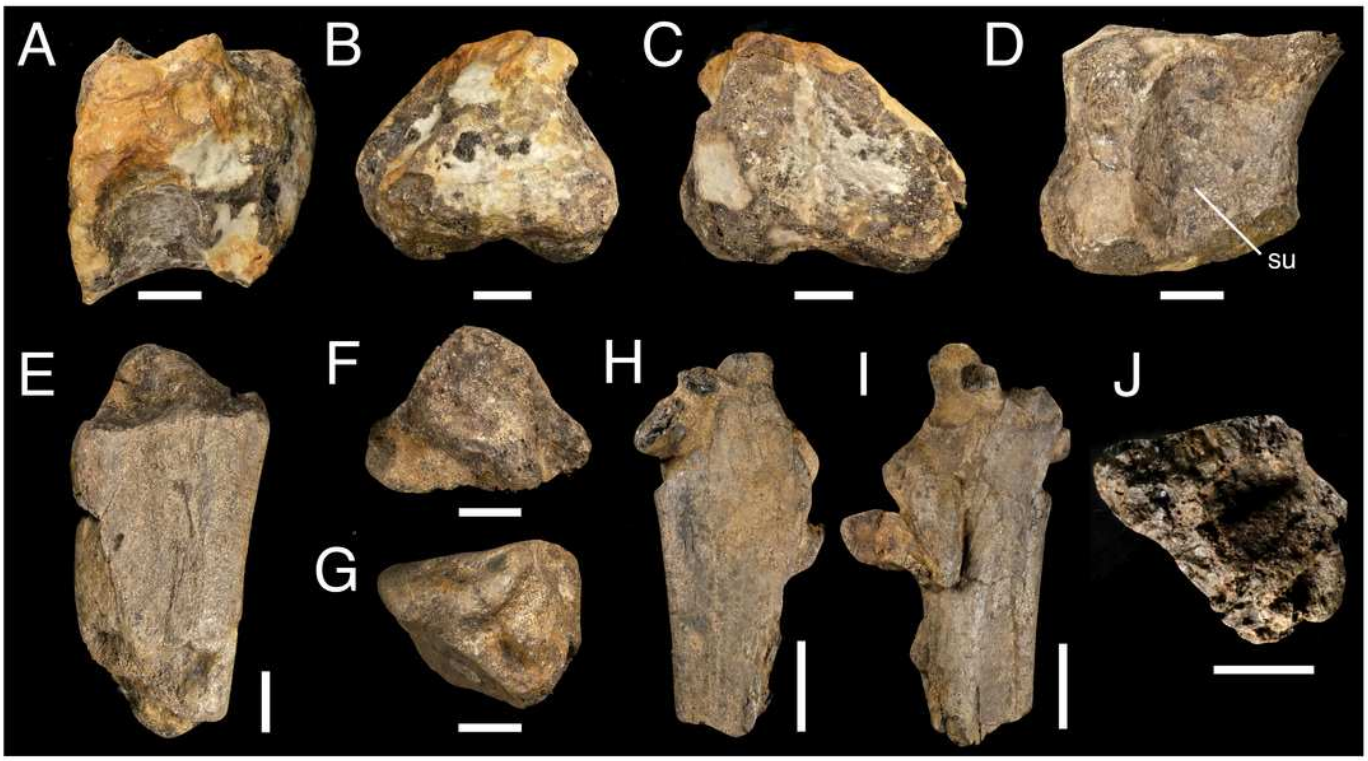

Figure 8

Fragmentary postacetabular process of the right ilium IWCMS 2018.30.7 (A, C, E, G, I) and 2018.30.8 (B, D, F, H, J)

(A–B) Medial view. (C–D) Ventrolateral oblique view. (E–F) Ventral view. (G–H) Anterior view. (I-J) Posterior view. *Abbreviations:*be, bioerosion; bf, brevis fossa; ll, lateral lamina; ml, medial lamina; nvf, neurovascular foramen. Scale bars: 50 mm.

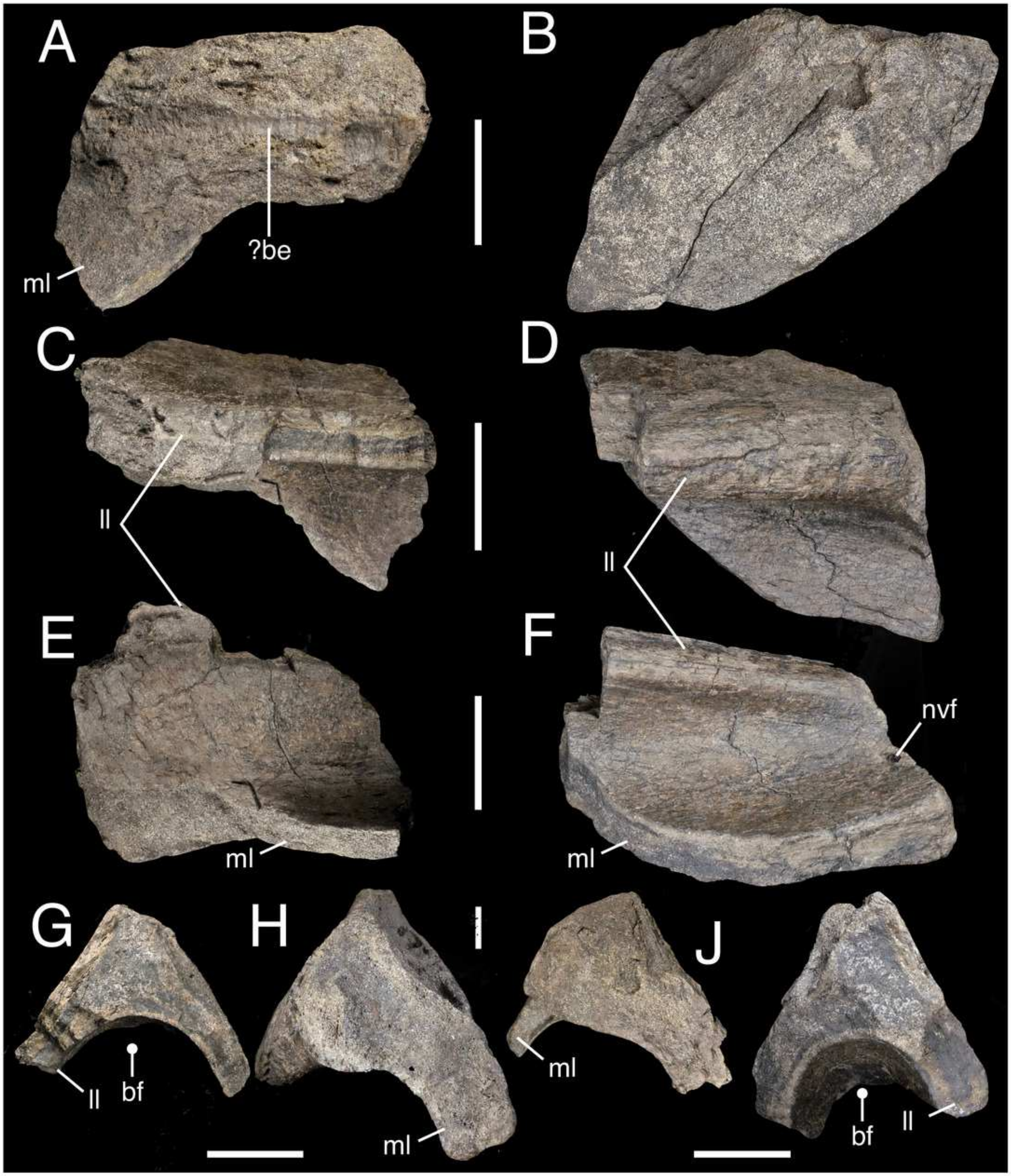
A
B
?be
ml
C
D
ll
ll
E
F
nvf
ml
ml
G
H
J
ll
bf
ml
ml
bf
ll

Figure 9

Long bone fragments IWCMS 2018.30.9 (A, B) and 2018.30.10 (C, D).

Views uncertain. *Abbreviations:*can, cancellous bone; cor, cortical bone. Scale bars: 50 mm.

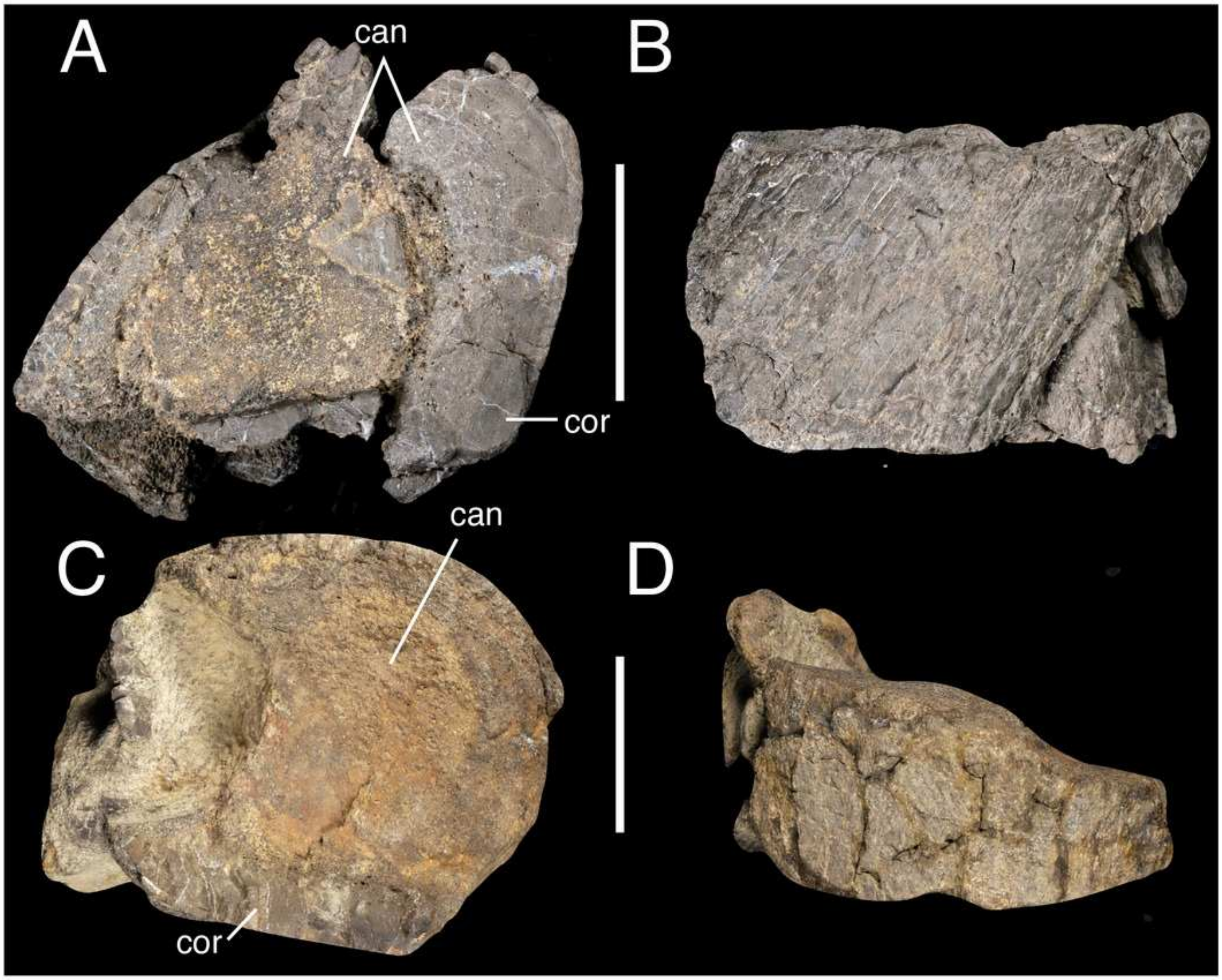
A
can
cor
B
C
can
cor
D

Figure 10

Bioeroded indeterminate bone fragment IWCMS 2018.30, displaying cross-sections of internal tubes.

Views uncertain. Figures F and G are counterparts. Asterisks denote continuation of a single tube visible in different views. *Abbreviations:*ca: cancellous bone; tu: tubes (preserved in cross-section). Scale bars: 50 mm (A–D); 20 mm (E–G).